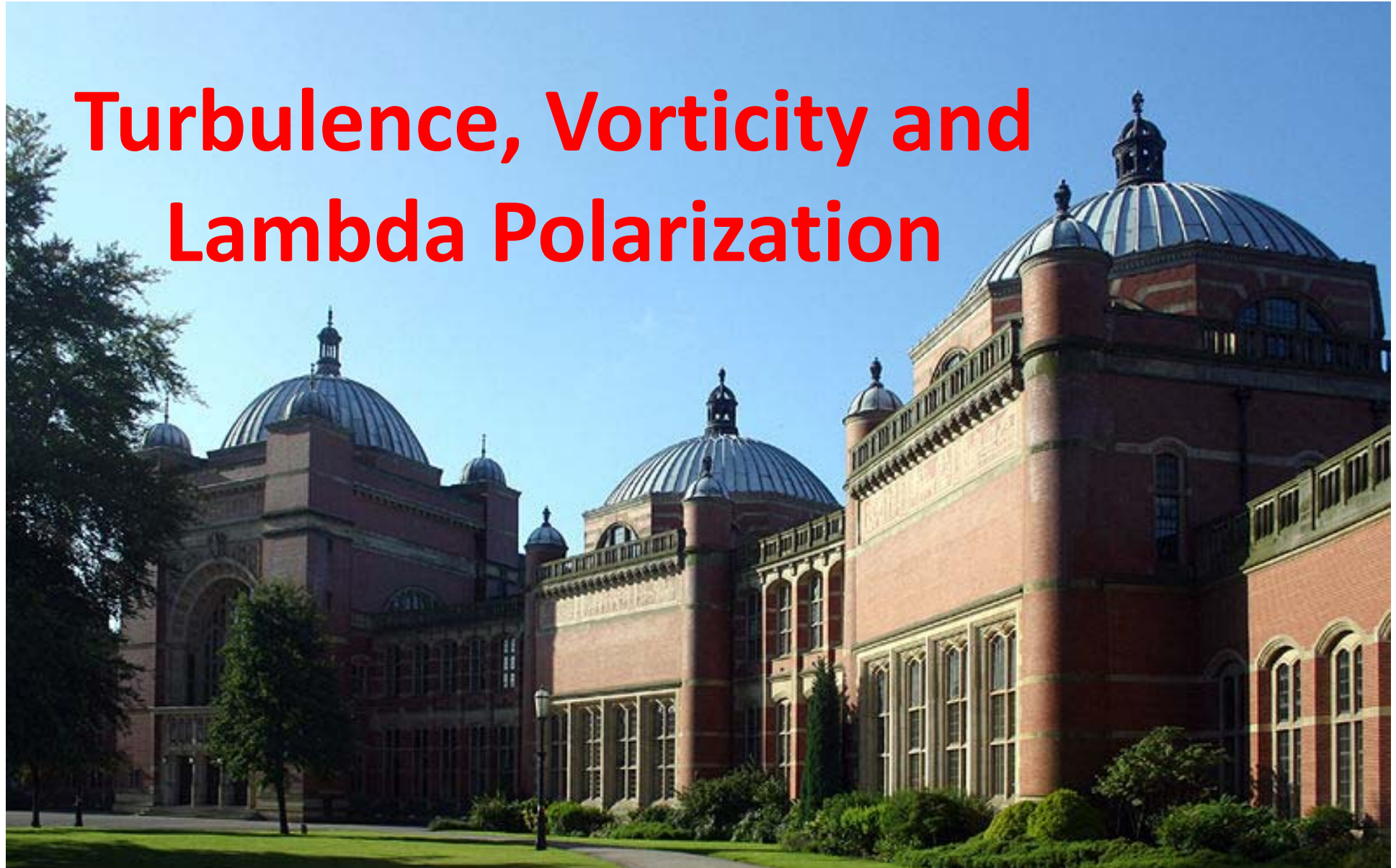


Turbulence, Vorticity and Lambda Polarization



Strangeness in Quark Matter SQM 2013
22nd - 27th July 2013 Birmingham, UK013

Laszlo P. Csernai,
University of Bergen, Norway

**Laszlo Pal Csernai,
Francesco Becattini,
Du-Juan Wang**

Strongly Interacting Low-Viscosity Matter Created in Relativistic Nuclear Collisions

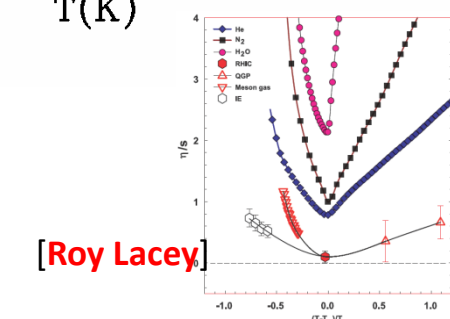
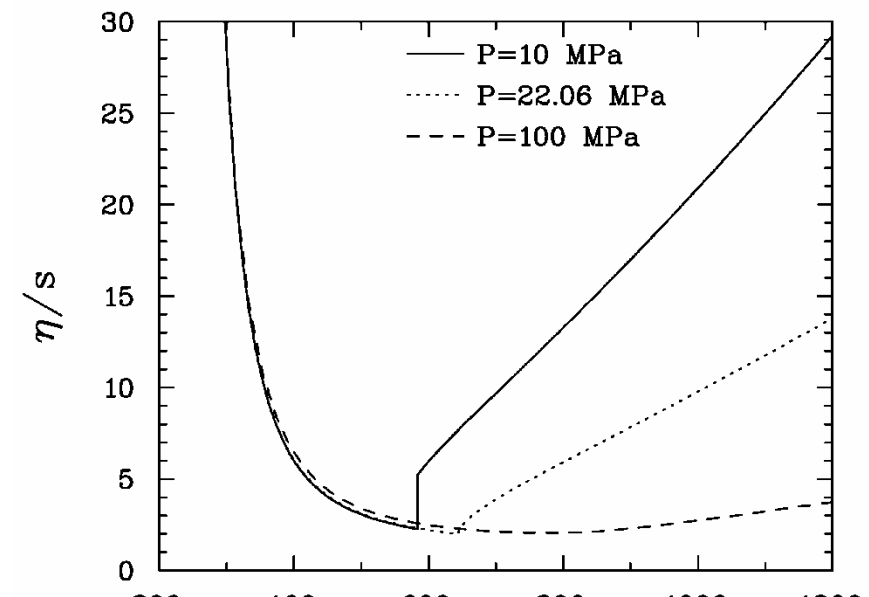
Laszlo P. Csernai,^{1,2} Joseph I. Kapusta,³ and Larry D. McLerran⁴

Due to low viscosity at the phase transition, several new phenomena occur in high energy Heavy Ion collisions:

- high multipolarity azimuthal fluctuations, up to v8,
- rotation (v1), shear, vorticity,
- Turbulence in the transverse and, reaction planes,
- Kelvin Helmholtz Instability (KHI).

These may lead to observable consequences:

- change of v1 flow
- Differential HBT
- Observable POLARIZATION of Λ and $\bar{\Lambda}$ in the reaction plane (x), pointing into the -y direction.



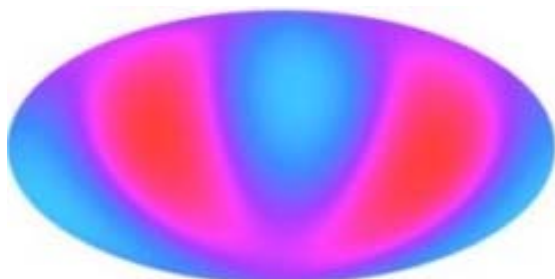
Low viscosity → Fluctuations



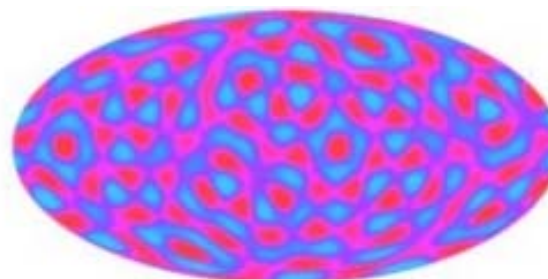
oil



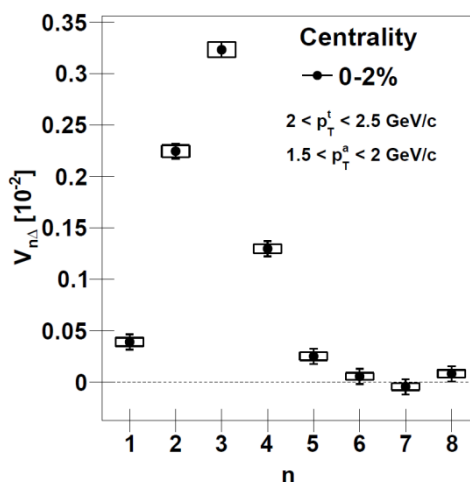
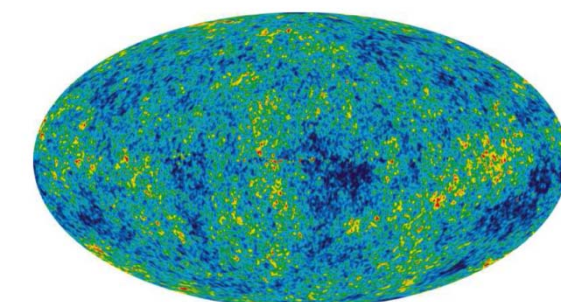
water



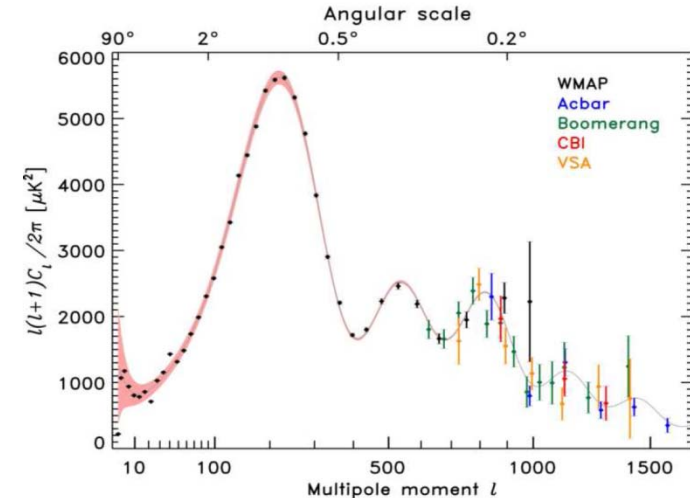
$\ell = 2$



$\ell = 16$



Measurable azimuthal
fluctuations up to $n=8$
are evidence for low
viscosity



The Cosmic Microwave Background as seen by Planck and WMAP

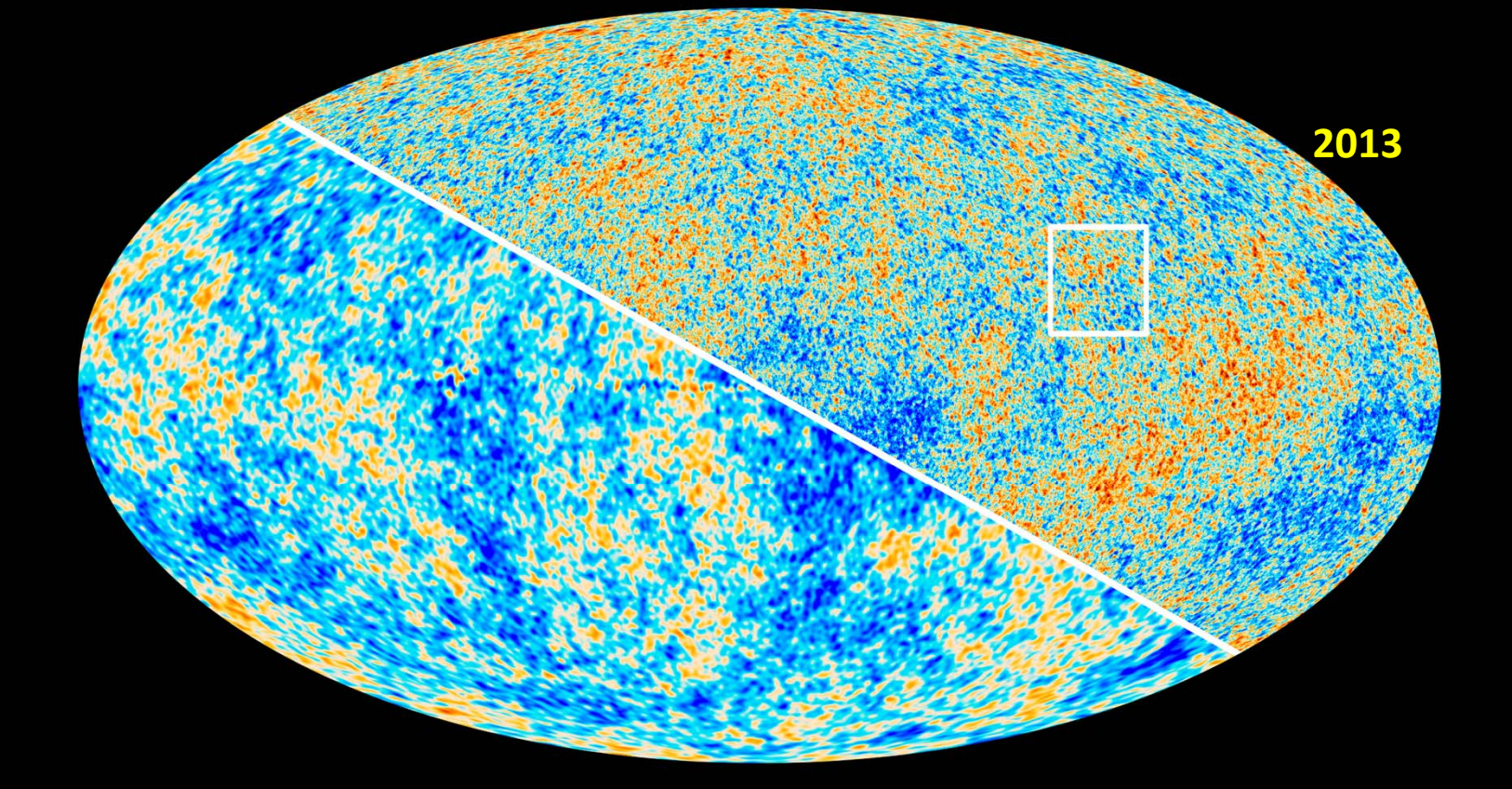


Figure 32: The CMB radiation temperature fluctuations from the 5-year WMAP data seen over the full sky. The average temperature is 2.725K, and the colors represents small temperature fluctuations. Red regions are warmer, and blue colder by about 0.0002 K.

Fluctuations form initial state only

QIN, PETERSEN, BASS, AND MÜLLER

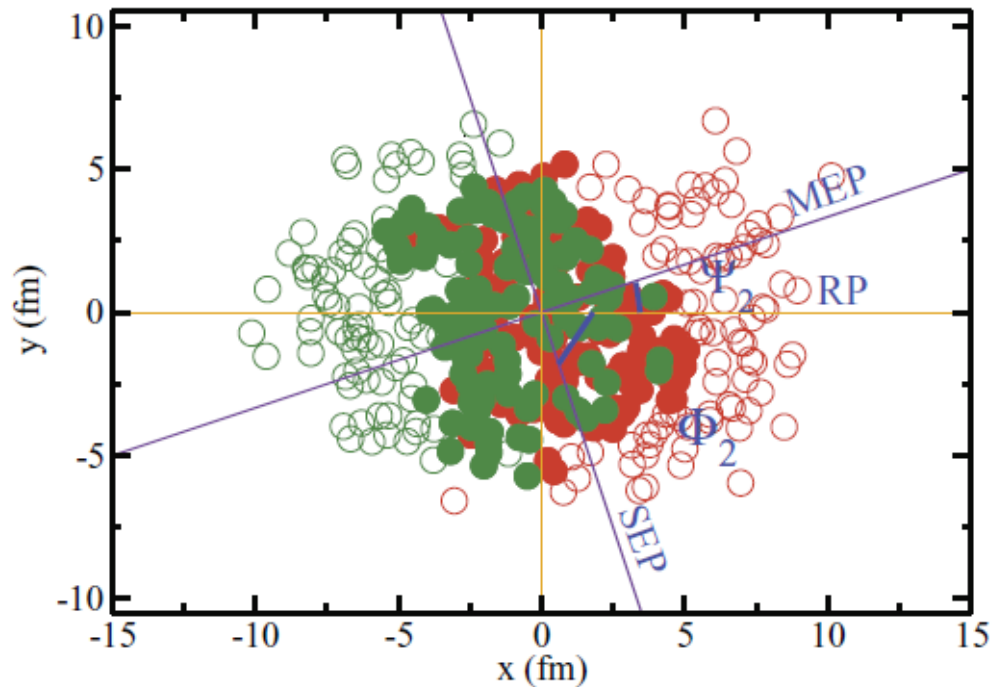


FIG. 3. (Color online) The transverse plane for one typical collision event, where the circles represent nucleons from two nuclei, with shaded ones for participating nucleons. Also shown are the locations of different planes: the reaction plane (RP), the spatial event plane (SEP), and the momentum event plane (MEP) for $n = 2$.

- [1] Gardim FG, Grassi F, Hama Y, Luzum M, Ollitrault PHYSICAL REVIEW C **83**, 064901 (2011); (v_1 also)
- [2] Qin GY, Petersen H, Bass SA, Mueller B PHYSICAL REVIEW C **82**, 064903 (2010)

Cumulative event planes show weak correlation with the global collective reaction plane (RP).

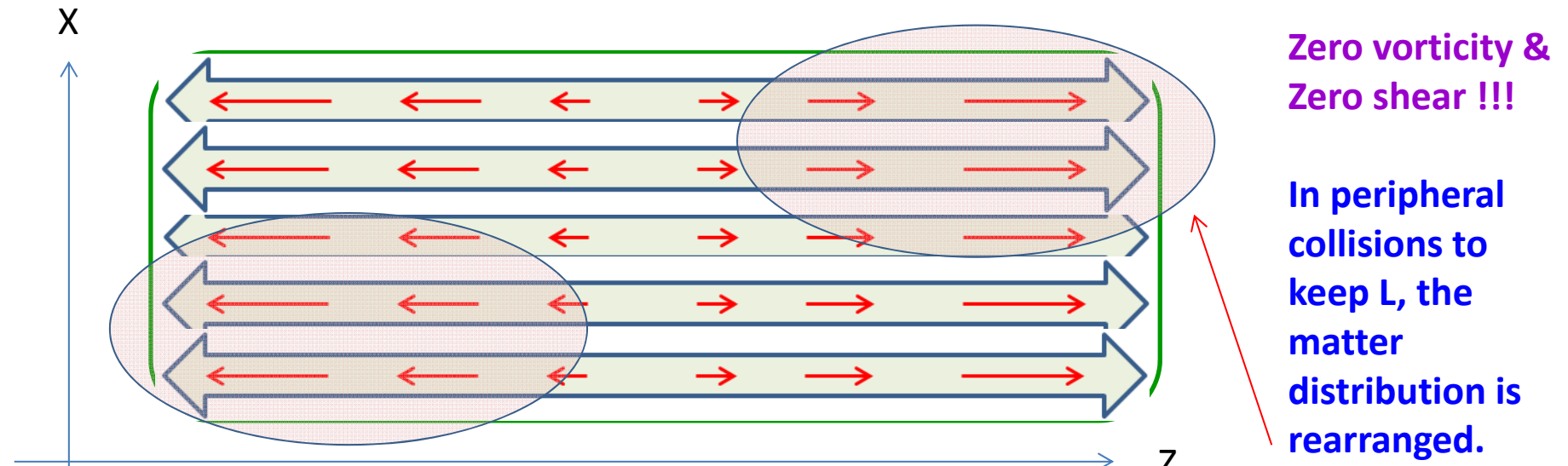
In [2] $v_1(pt)$ is analyzed (for RHIC) and the azimuthal shape spectrum is arising from initial state shape fluctuations. (!!!)

No room for critical fluctuations ?
[J. Kapusta & B. Mueller]

Typical I.S. model – scaling flow

The same longitudinal expansion velocity profile in the whole [x,y]-plane !
 No shear flow. **No string tension!** Usually **angular momentum is vanishing!**

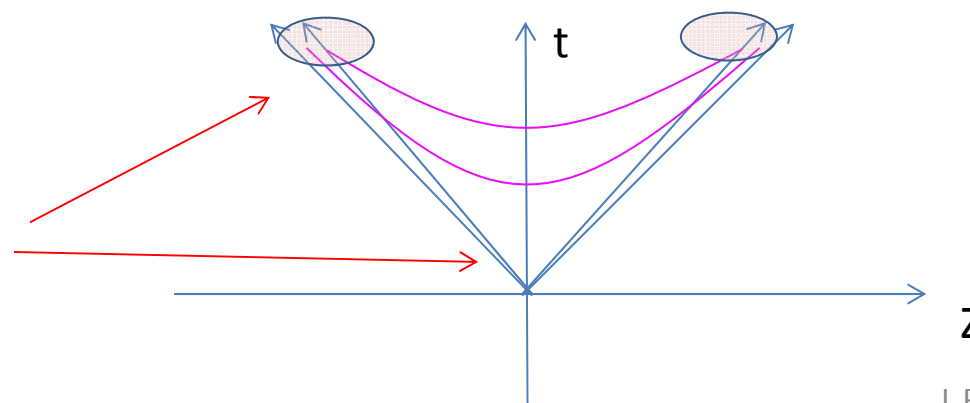
$$\omega_y \equiv \omega_{xz} \equiv -\omega_{zx} \equiv \frac{1}{2}(\partial_z v_x - \partial_x v_z) \quad \omega \equiv \frac{1}{2} \text{rot } \mathbf{v} = \frac{1}{2} \nabla \times \mathbf{v}$$



Zero vorticity & Zero shear !!!

In peripheral collisions to keep L, the matter distribution is rearranged.

Such a re-arrangement of the matter density is dynamically not possible in a short time!



Adil & Gyulassy (2005) initial state

x, y, η, τ coordinates → Bjorken scaling flow

PHYSICAL REVIEW C 72, 034907 (2005)

Considering a longitudinal “*local relative rapidity slope*”, based on observations in D+Au collisions:

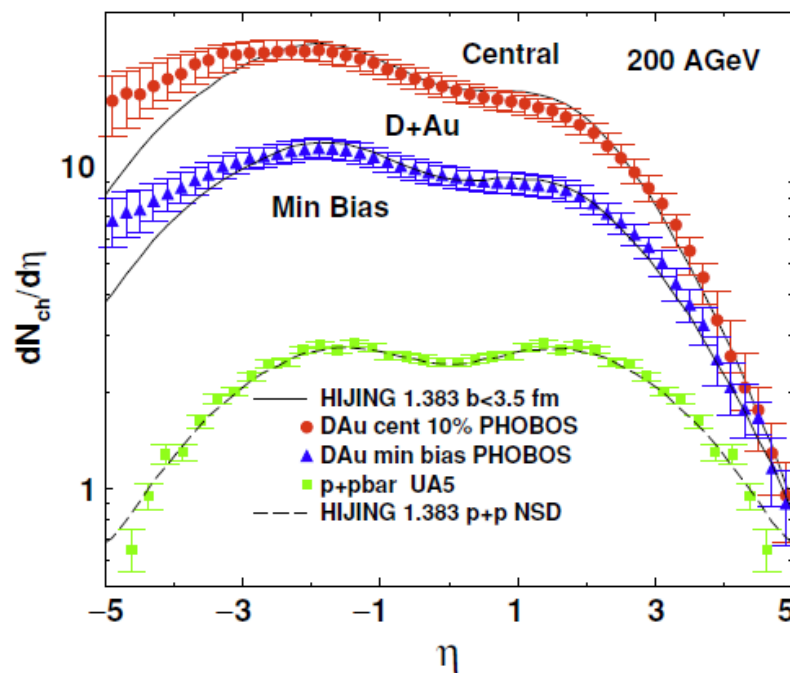
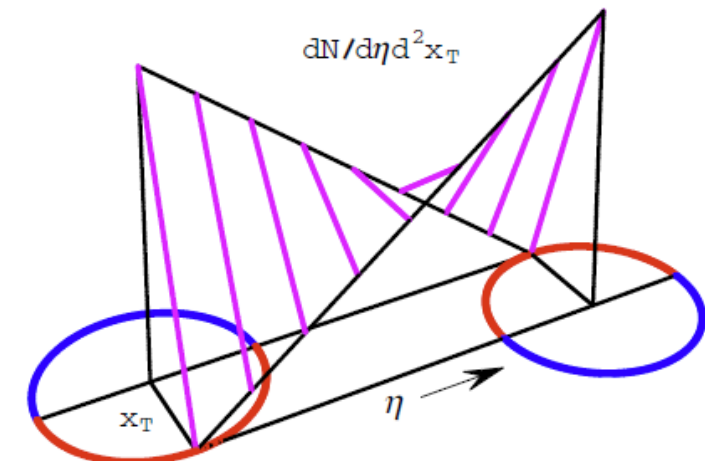


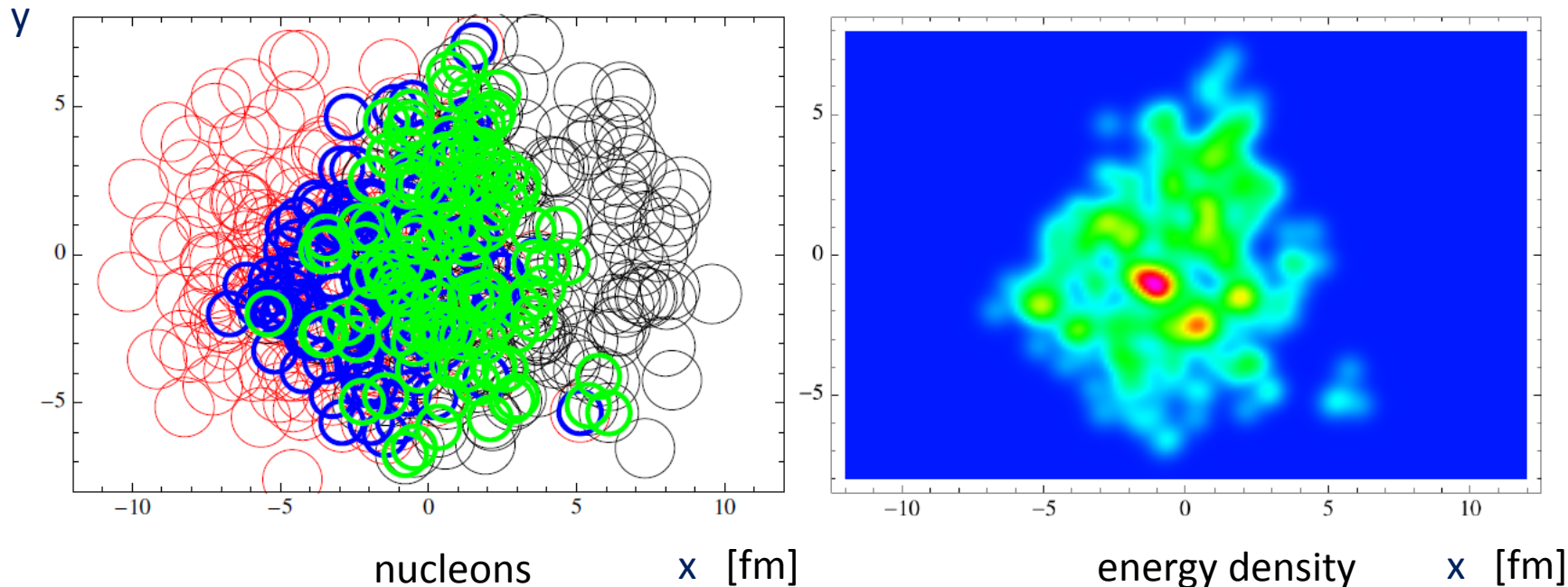
FIG. 2. (Color online) Asymmetric pseudorapidity distributions of charged hadrons produced in D+Au minimum bias and central 0–10% reactions at 200A GeV from PHOBOS [12] are compared to $p+\bar{p}$ data from UA5 [13]. The curves show predictions using the HIJING v1.383 code [14,15].



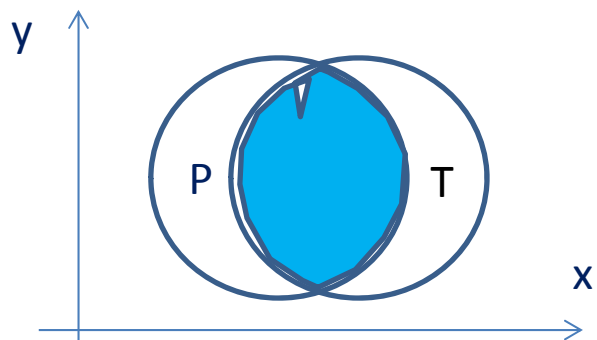
Led to directed flow v_1 at RHIC energies instead of antiflow.

Onset of turbulence around the Bjorken flow

S. Floerchinger & U. A. Wiedemann, JHEP 1111:100, 2011; arXiv: 1108.5535v1



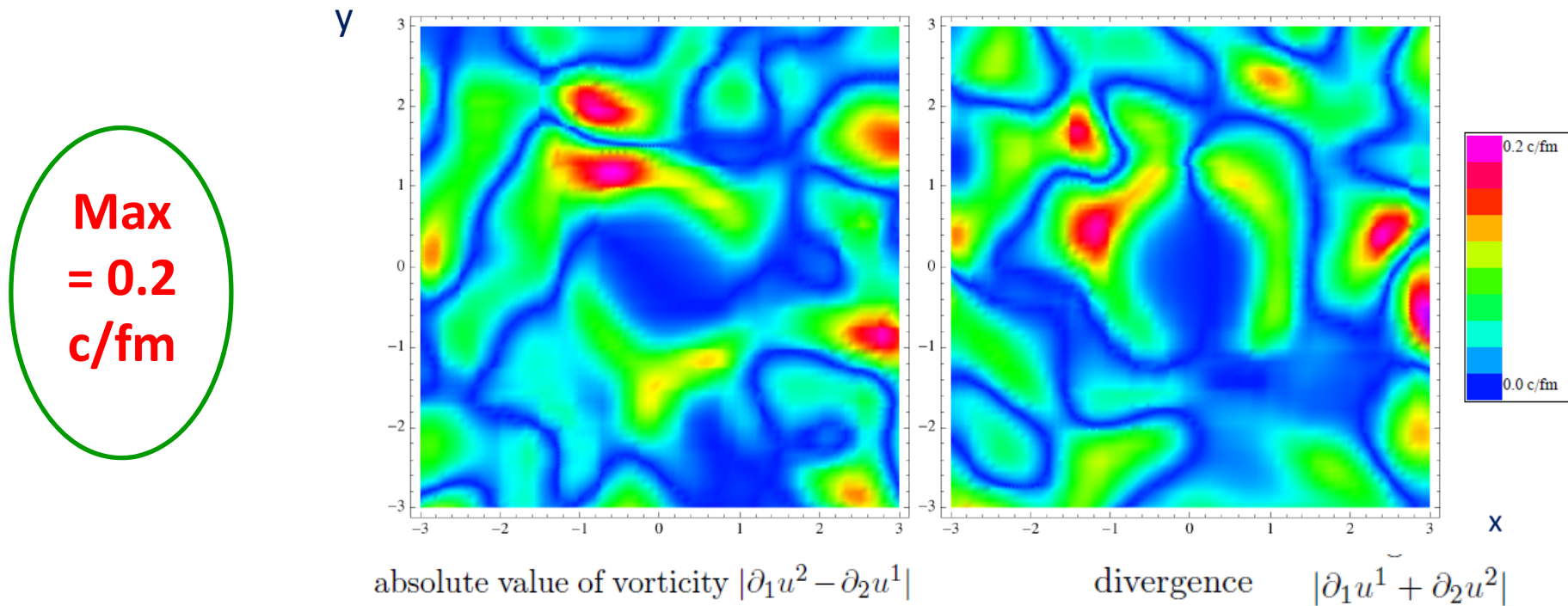
- Transverse plane [x,y] of a Pb+Pb HI collision at $\sqrt{s}_{NN}=2.76\text{TeV}$ at $b=6\text{fm}$ impact parameter
- Longitudinally [z]: **uniform** Bjorken flow, (expansion to infinity), depending on τ only.



Green and **blue** have the same longitudinal speed (!) in this model.
Longitudinal shear flow is omitted.

Onset of turbulence around the Bjorken flow

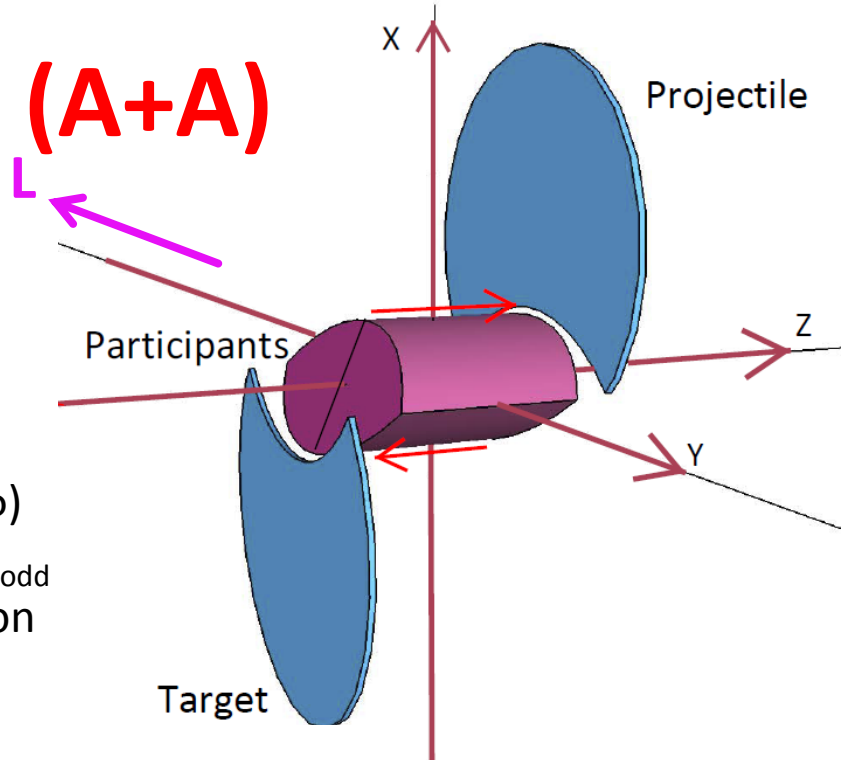
S. Floerchinger & U. A. Wiedemann, JHEP 1111:100, 2011; arXiv: 1108.5535v1



- Initial state Event by Event vorticity and divergence fluctuations.
- Amplitude of random vorticity and divergence fluctuations are the same
- In dynamical development viscous corrections are negligible (\rightarrow no damping)
- Initial transverse expansion in the middle ($\pm 3\text{fm}$) is neglected (\rightarrow no damping)
- High frequency, high wave number fluctuations **may feed** lower wave numbers

Peripheral Collisions (A+A)

- Global Symmetries
- Symmetry axes in the global CM-frame:
 - ($y \leftrightarrow -y$)
 - ($x, z \leftrightarrow -x, -z$)
 - Azimuthal symmetry: ϕ -even ($\cos n\phi$)
 - Longitudinal z -odd, (rap.-odd) for v_{odd}
 - Spherical or ellipsoidal flow, expansion



$$\frac{d^3N}{dydp_t d\phi} = \frac{1}{2\pi} \frac{d^2N}{dydp_t} [1 + 2v_1(y, p_t) \cos(\phi) + 2v_2(y, p_t) \cos(2\phi) + \dots]$$

$$\frac{d^3N}{dydp_t d\phi} = \frac{1}{2\pi} \frac{d^2N}{dydp_t} [1 + 2v_1(y - \underline{y}_{CM}, p_t) \cos(\phi - \underline{\Psi}_{RP}) + 2v_2(y - \underline{y}_{CM}, p_t) \cos(2(\phi - \underline{\Psi}_{RP})) + \dots]$$

L. P. Csernai,¹ G. Eyyubova,^{2,3} and V. K. Magas⁴
 PHYSICAL REVIEW C 86, 024912 (2012)

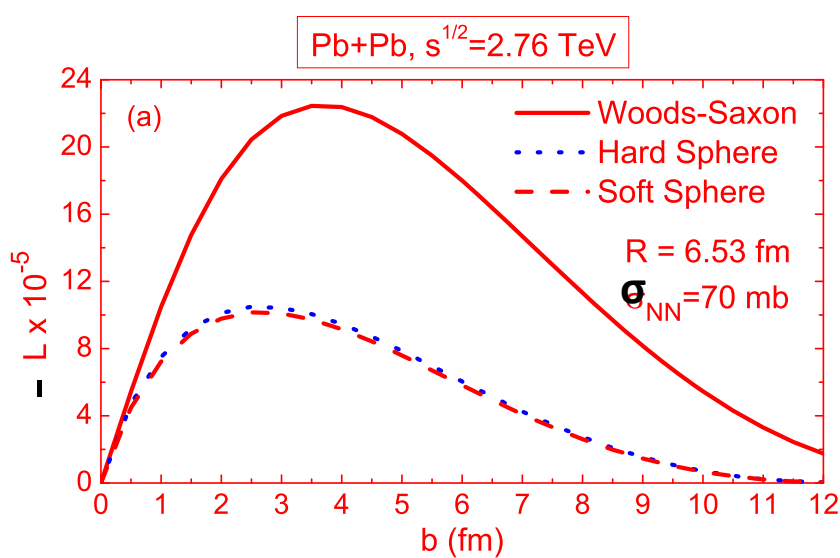
- Fluctuations
- Global flow and Fluctuations are simultaneously present $\rightarrow \exists$ interference
 - Azimuth - Global: even harmonics - Fluctuations : odd & even harmonics
 - Longitudinal – Global: v_1, v_3 y -odd - Fluctuations : odd & even harmonics
 - The separation of Global & Fluctuating flow is a must !! (not done yet)

Global Flow in Peripheral Collisions (A+A)

- Many interesting phenomena:
 - Historically: Bounce off / Side splash; Squeeze out → pressure & EoS
 - 3rd flow or Anti-flow (QGP), Rotation, KHI, Polarization, etc
 - These occur only if viscosity is low! → viscosity
- With increasing energy flow becomes strongly F/B directed & v_1 decreases

Initial States:

Detecting initial rotation

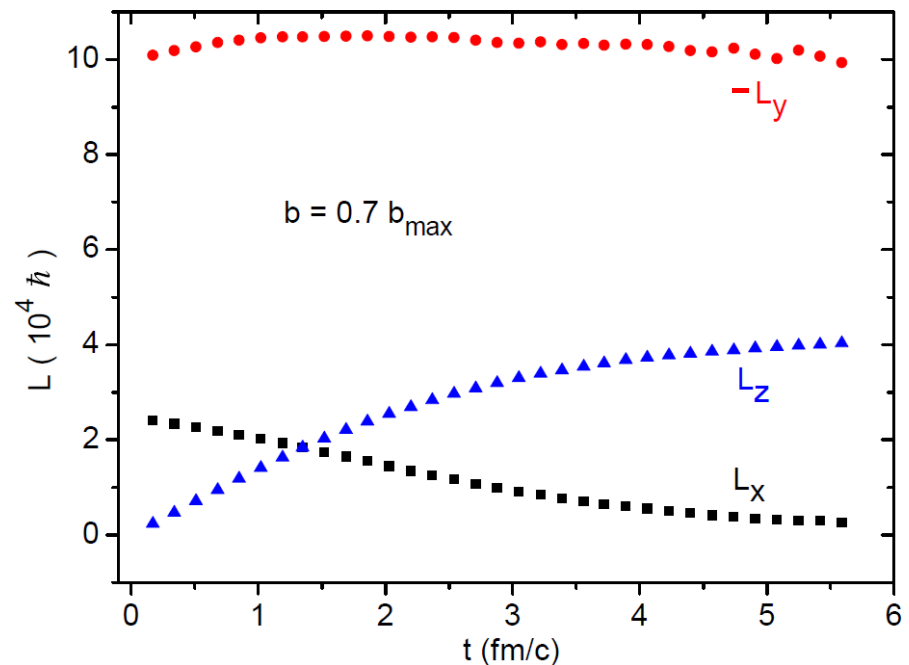


V. Vovchenko,¹ D. Anchishkin,² and L. P. Csernai³

PHYSICAL REVIEW C 88, 014901 (2013)

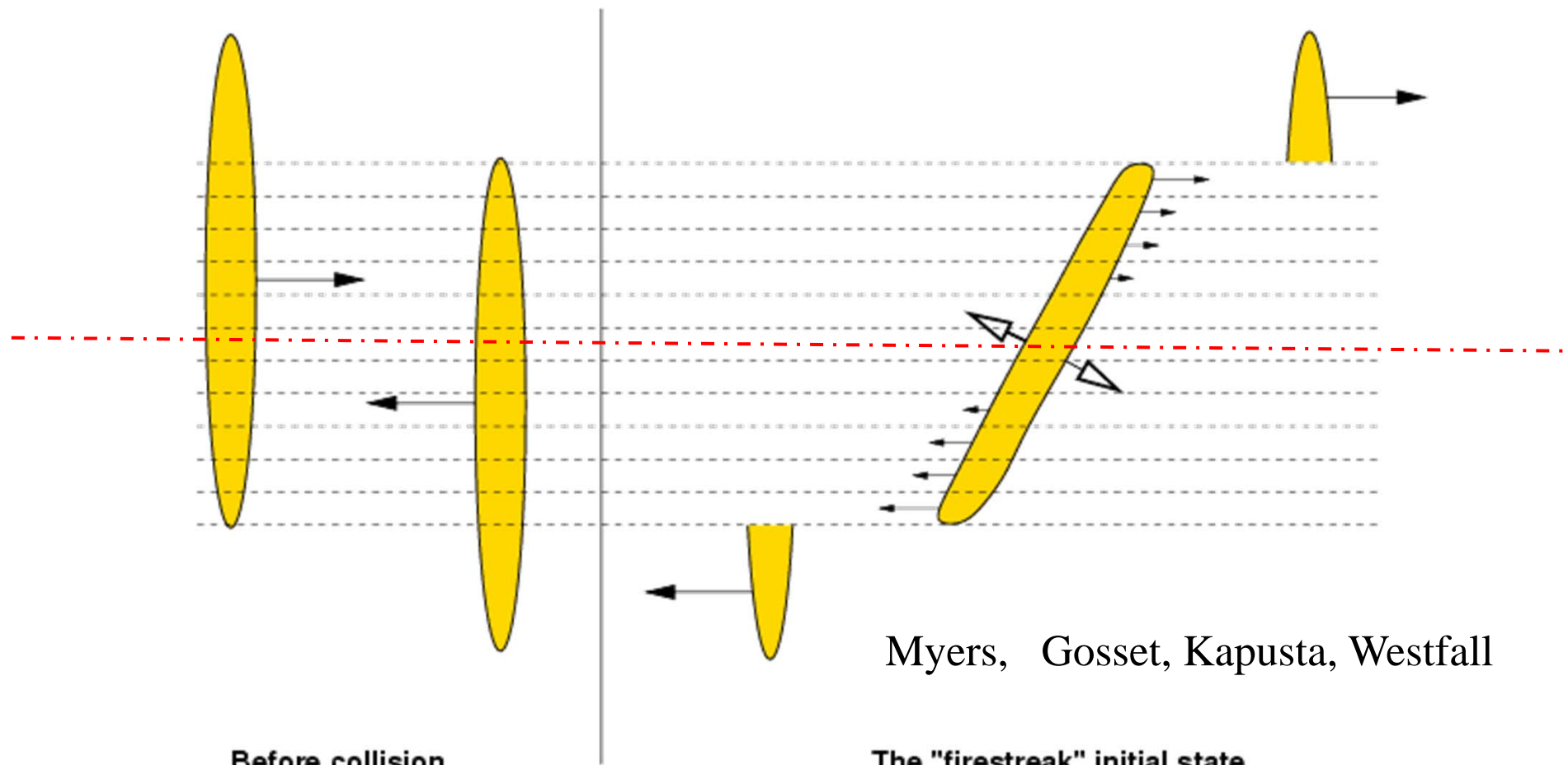
J. H. Gao, S. W. Chen, W. T. Deng, Z. T. Liang, Q. Wang and X. N. Wang, Phys. Rev. C 77, 044902 (2008).

F. Becattini, F. Piccinini, J. Rizzo, Phys. Rev. C 77, 024906 (2008).



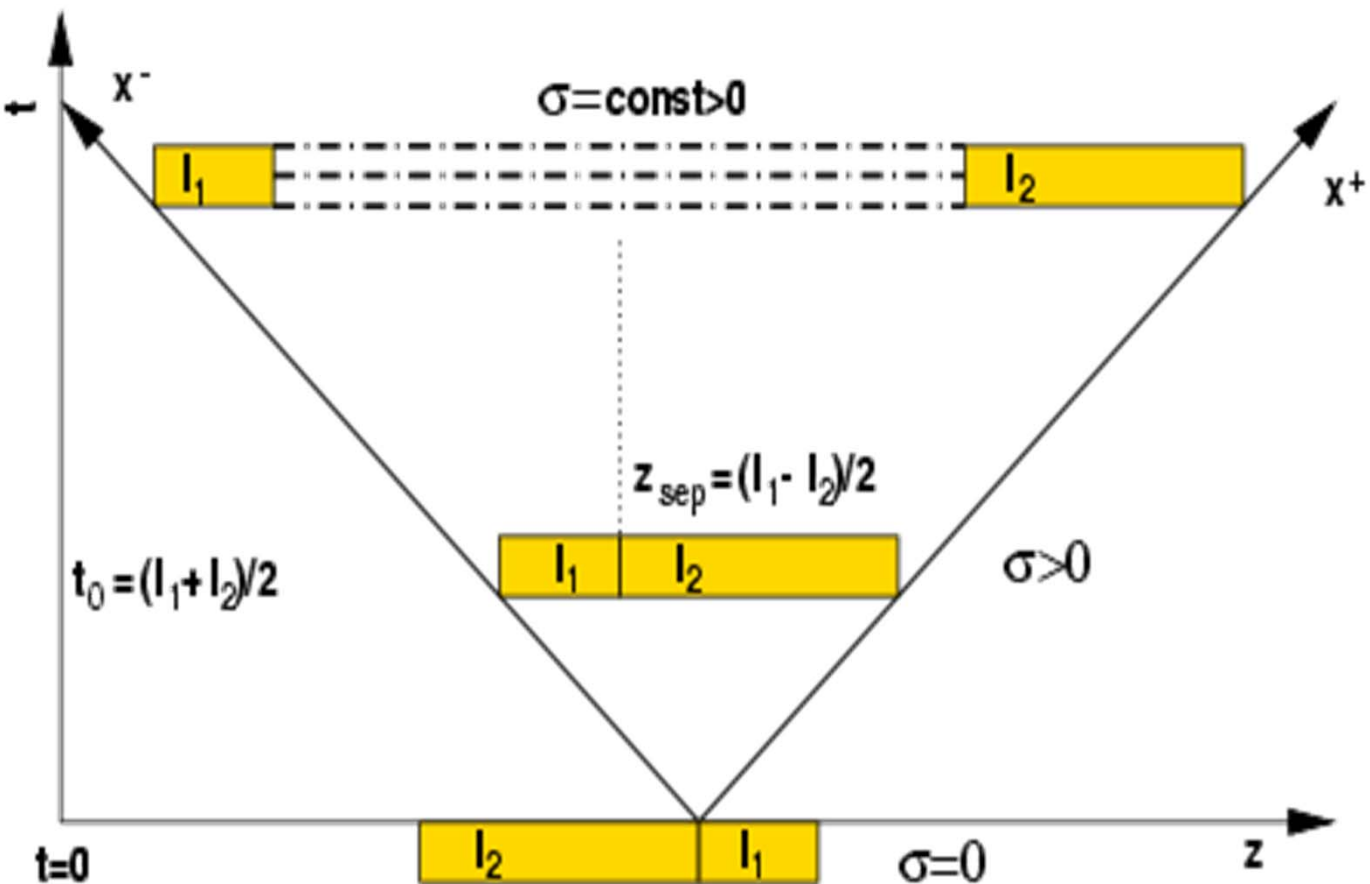
Angular momentum in the positive y half space (therefore L_x and L_z do not vanish).

„Fire streak“ picture – 3 dim.

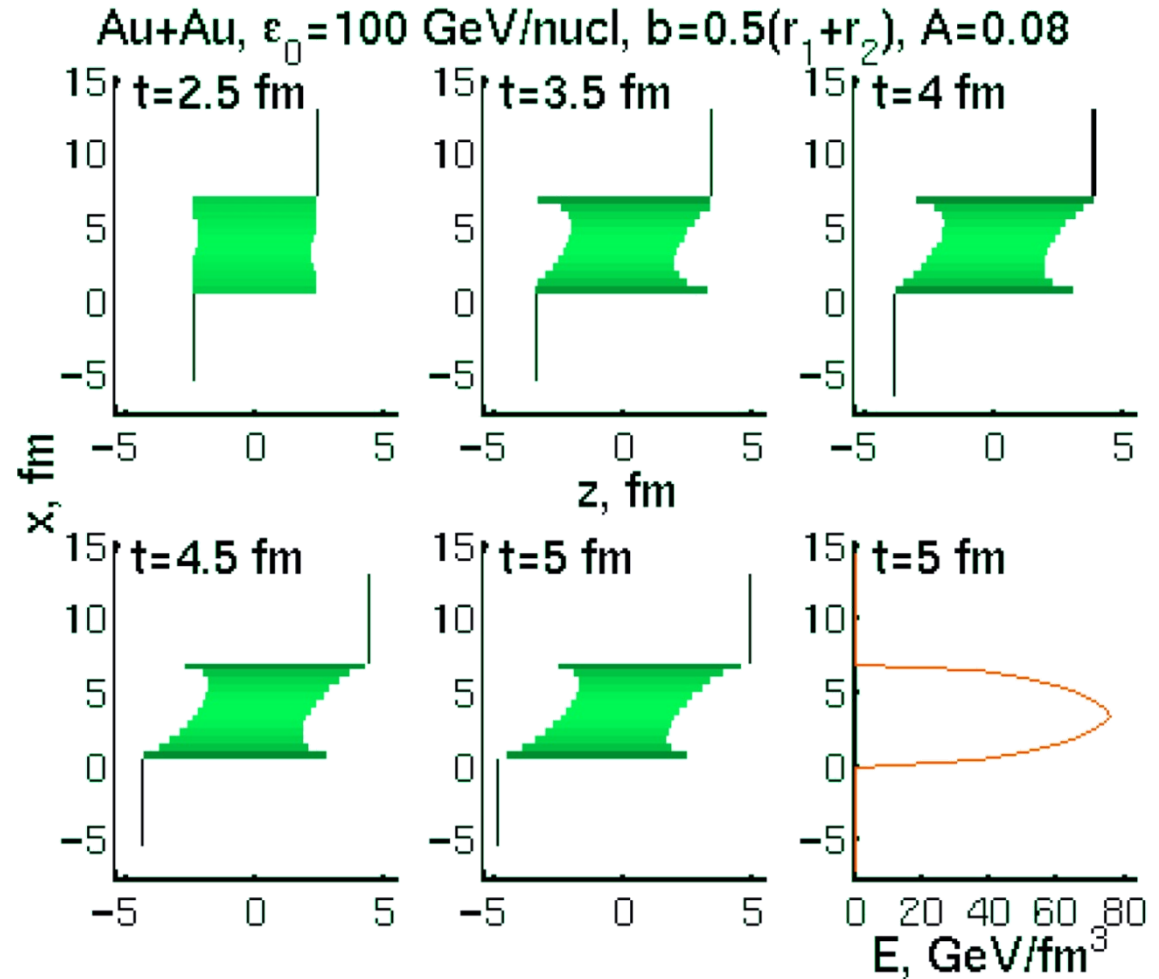
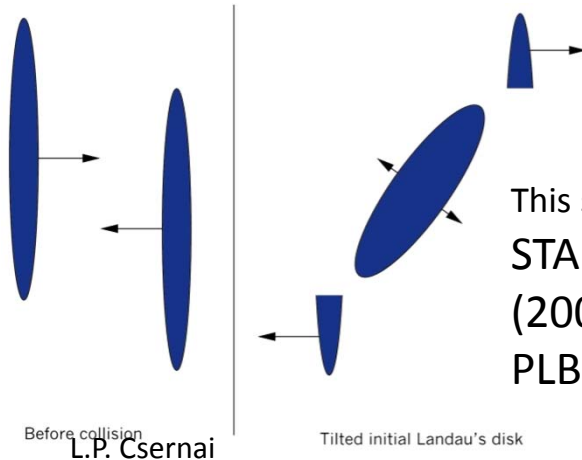


Symmetry axis = z-axis. Transverse plane divided into streaks.

String rope --- Flux tube --- Coherent YM field



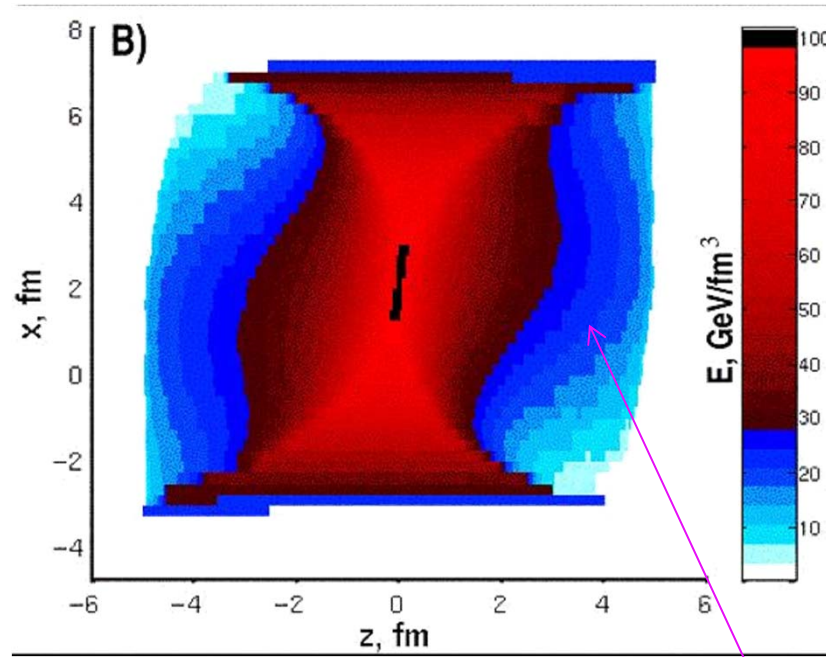
Initial State



This shape is confirmed by
STAR HBT: PLB496
(2000) 1; & M.Lisa &al.
PLB 489 (2000) 287.

3rd flow component

Initial state – reaching equilibrium



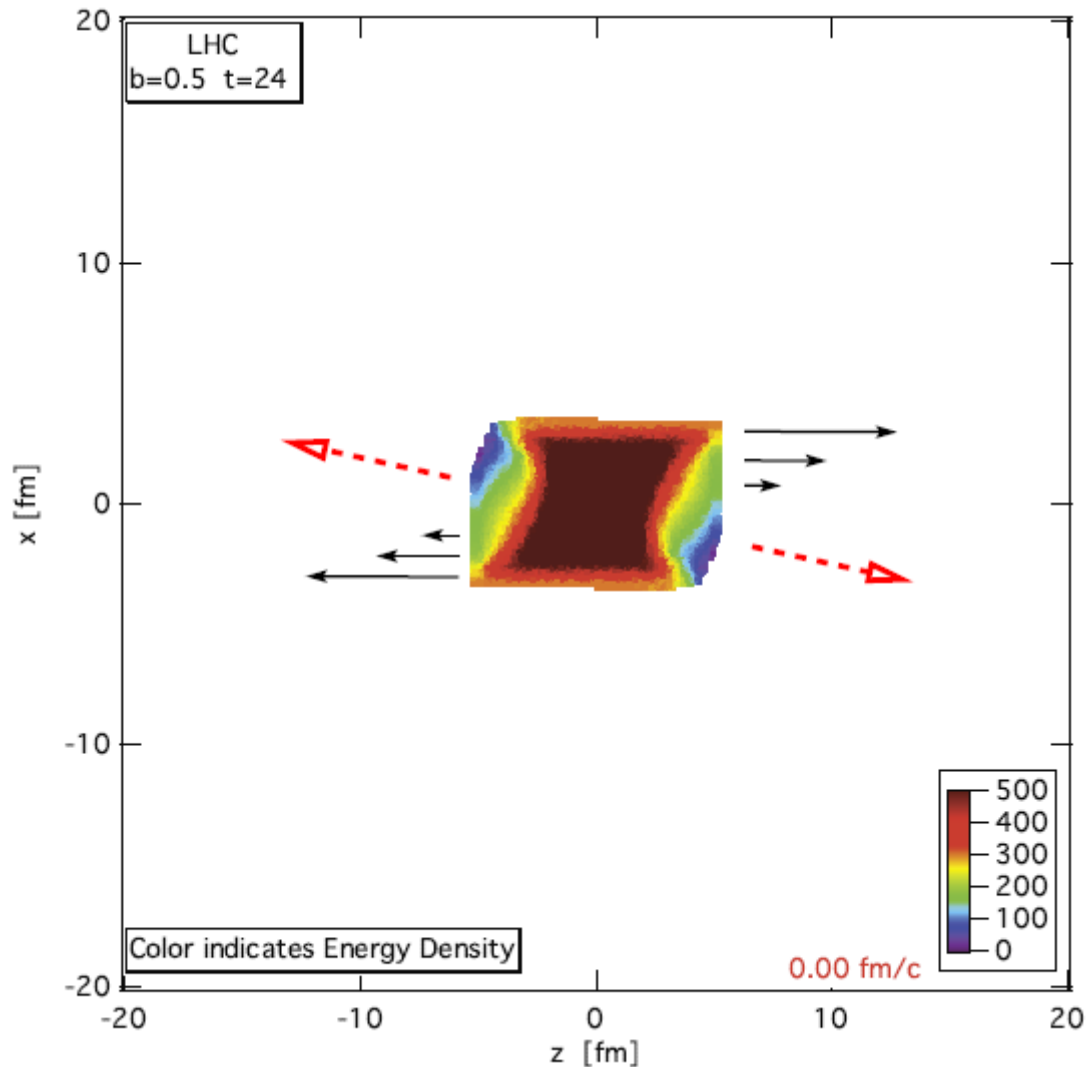
Initial state by V. Magas, L.P.

Csernai and D. Strottman

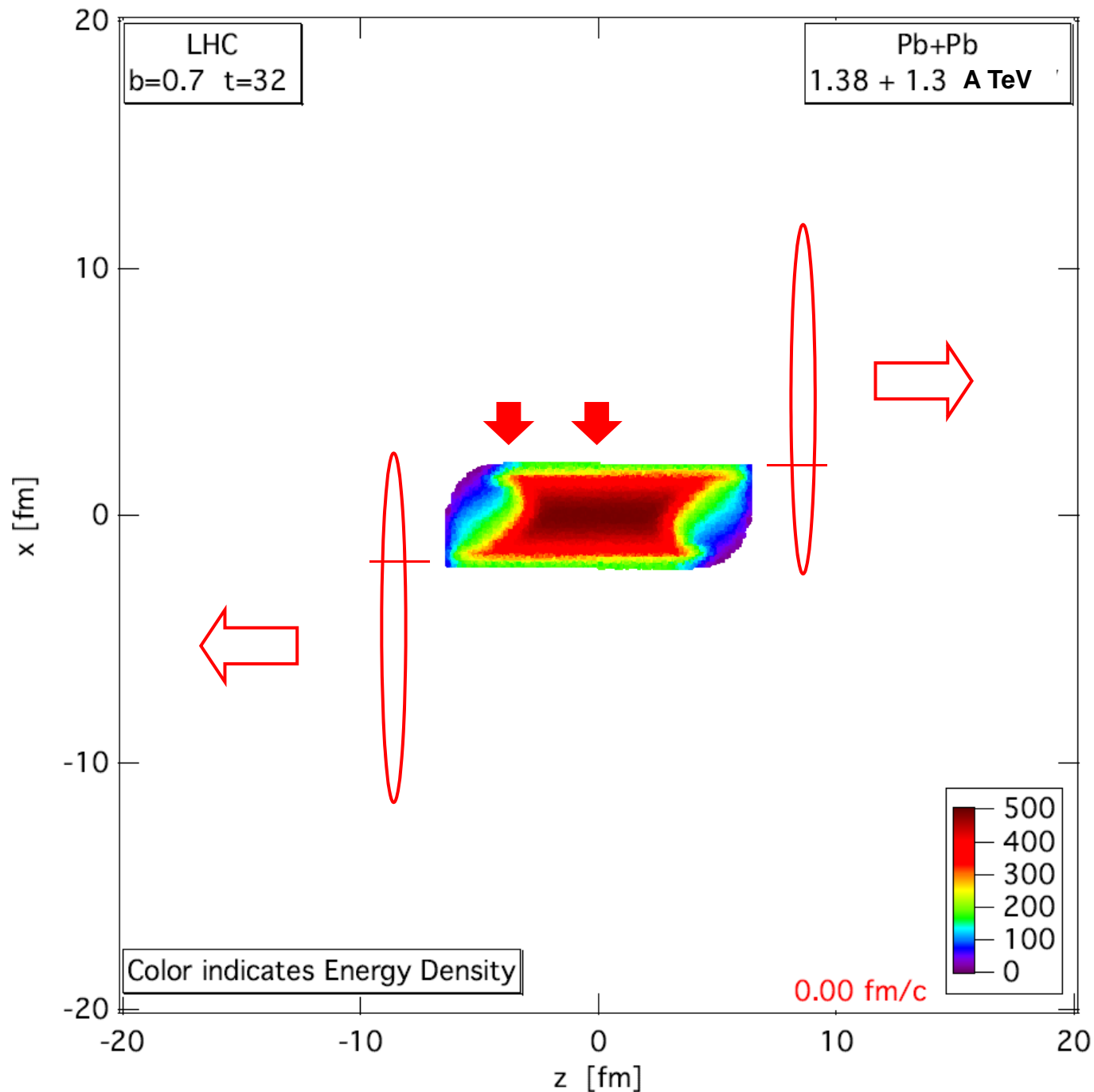
Phys. Rev. C64 (01) 014901;
Nucl. Phys. A 712 (02) 167.

Relativistic, 1D Riemann
expansion is added to
each stopped streak

Anti-flow (v_1) at LHC



Initial energy density [GeV/fm³] distribution in the reaction plane, [x,y] for a Pb+Pb reaction at 1.38 + 1.38 ATeV collision energy and impact parameter $b = 0.5 \cdot b_{\max}$ at time 4 fm/c after the first touch of the colliding nuclei, this is when the hydro stage begins. The calculations are performed according to the effective string rope model. This tilted initial state has a flow velocity distribution, qualitatively shown by the arrows. The dashed arrows indicate the direction of the largest pressure gradient at this given moment.



PIC-hydro

Pb+Pb 1.38+1.38 A TeV, $b = 70\%$ of b_{max}

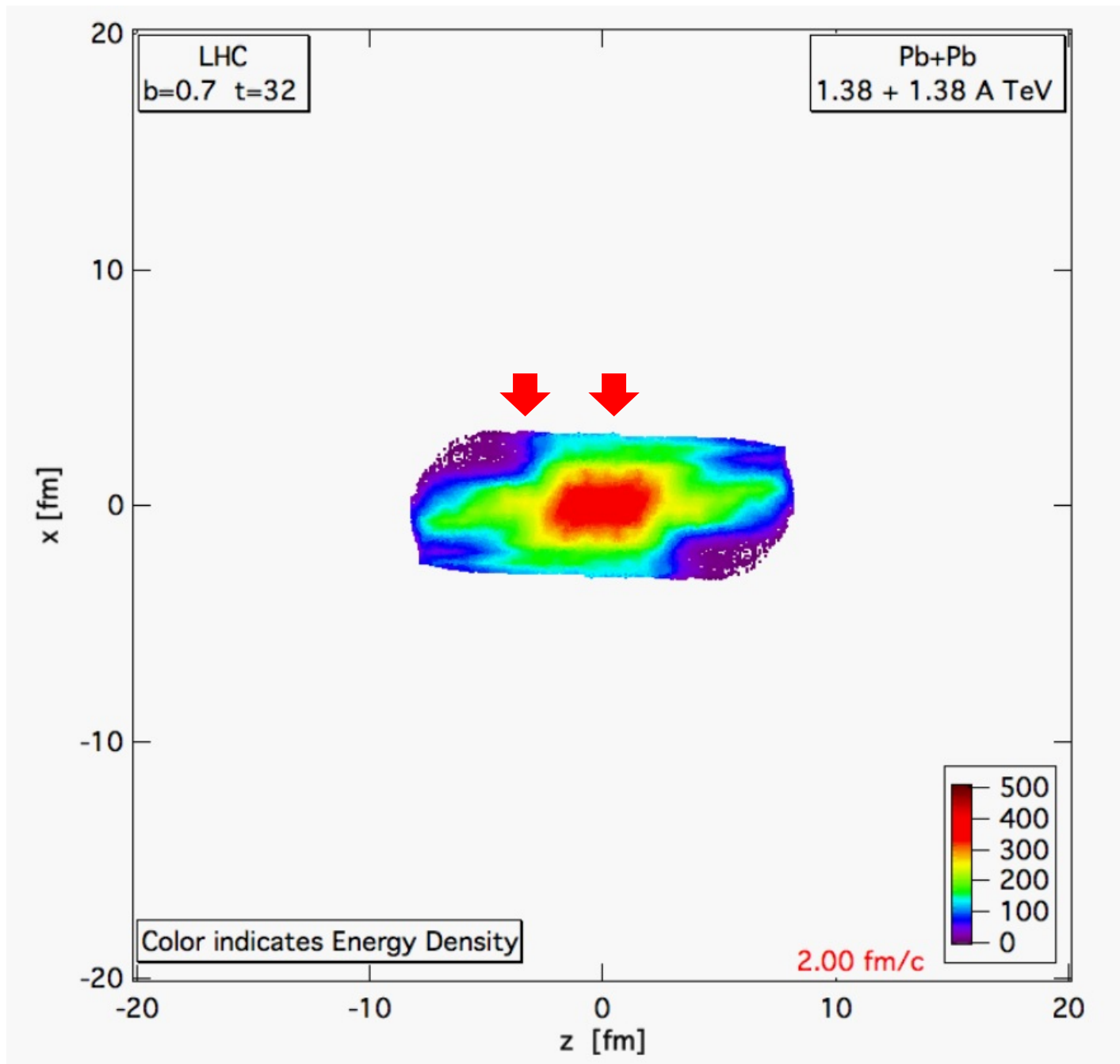
Lagrangian fluid cells, moving, ~ 5 mill.

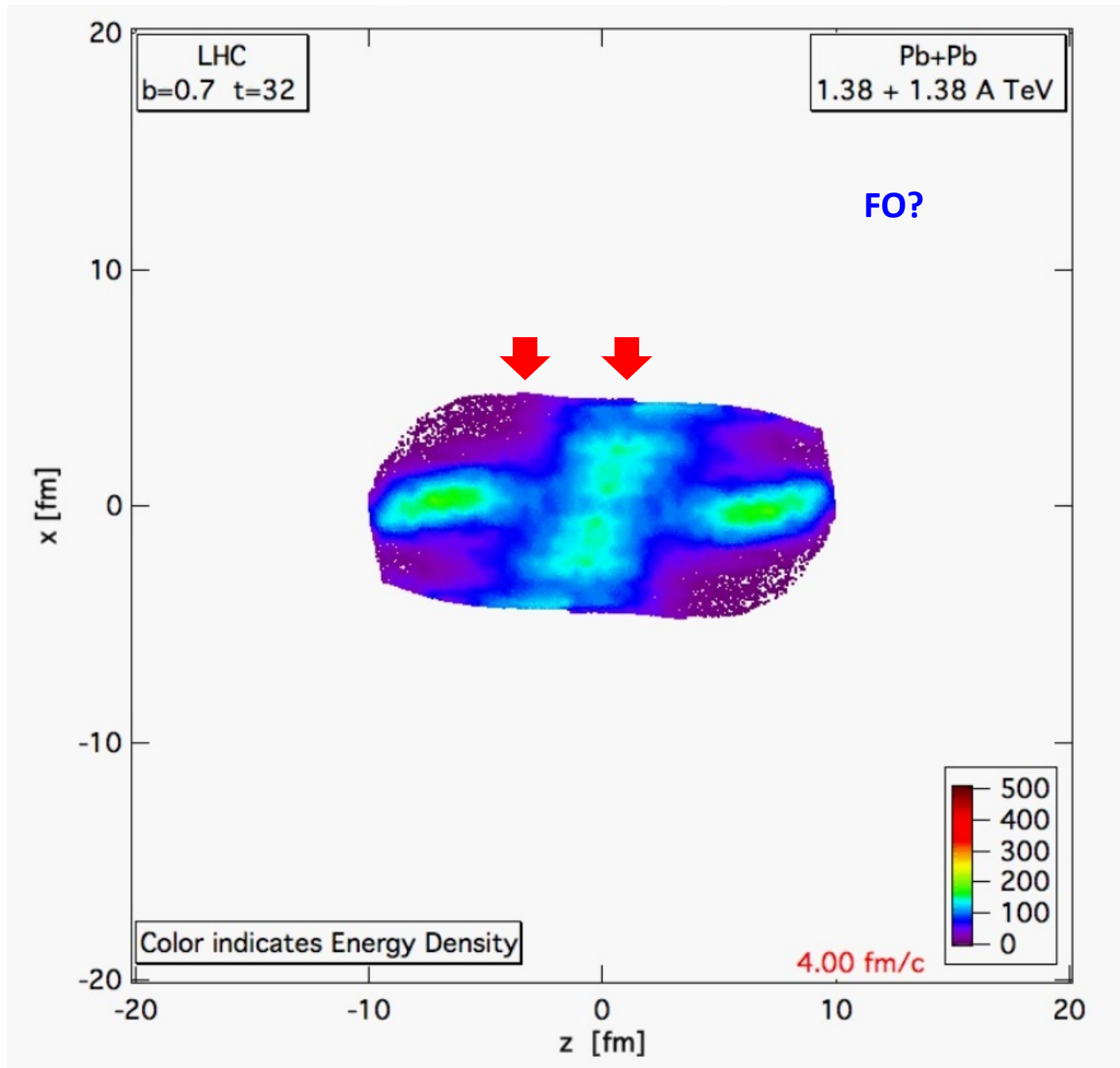
MIT Bag m. EoS

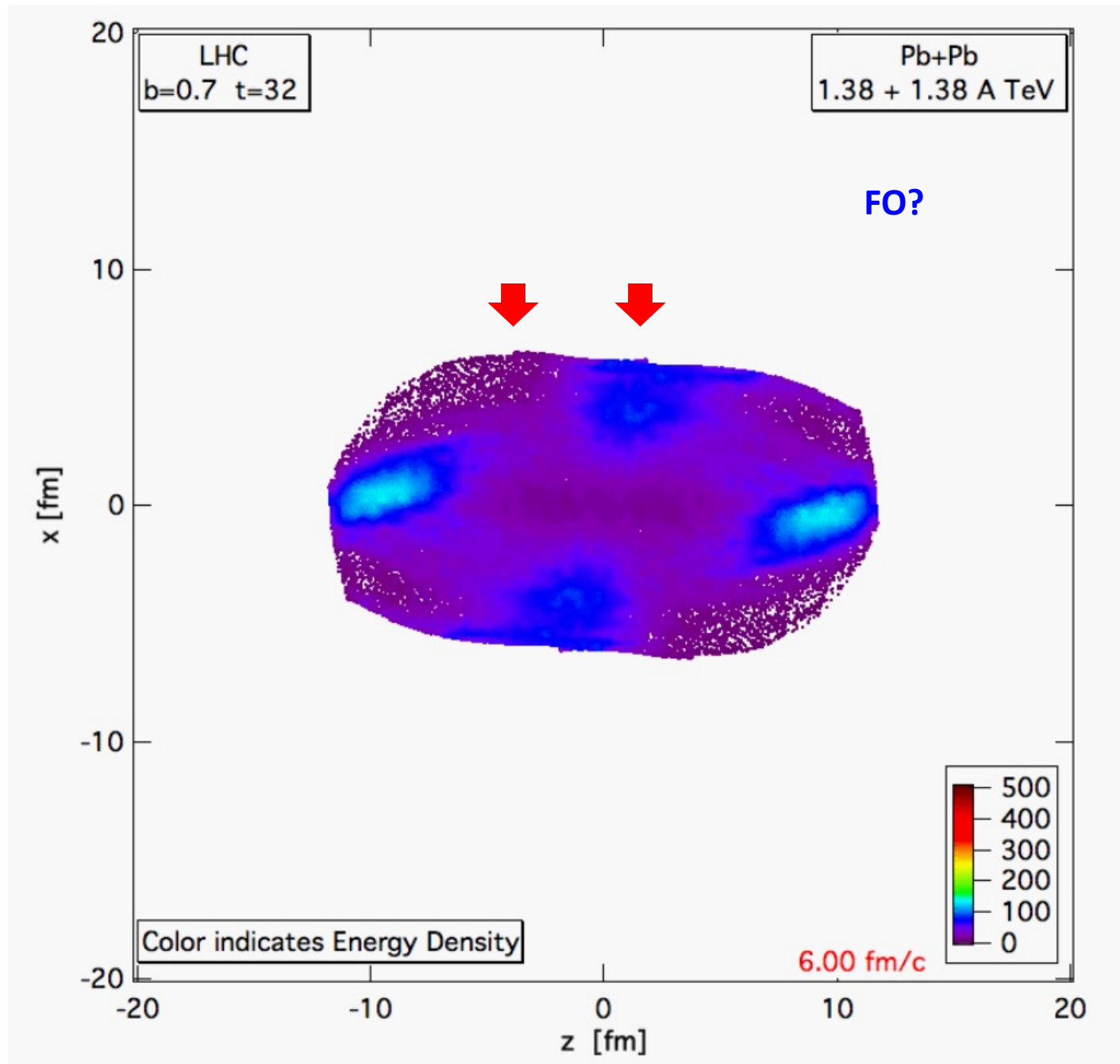
FO at $T \sim 200$ MeV, but calculated much longer, until pressure is zero for 90% of the cells.

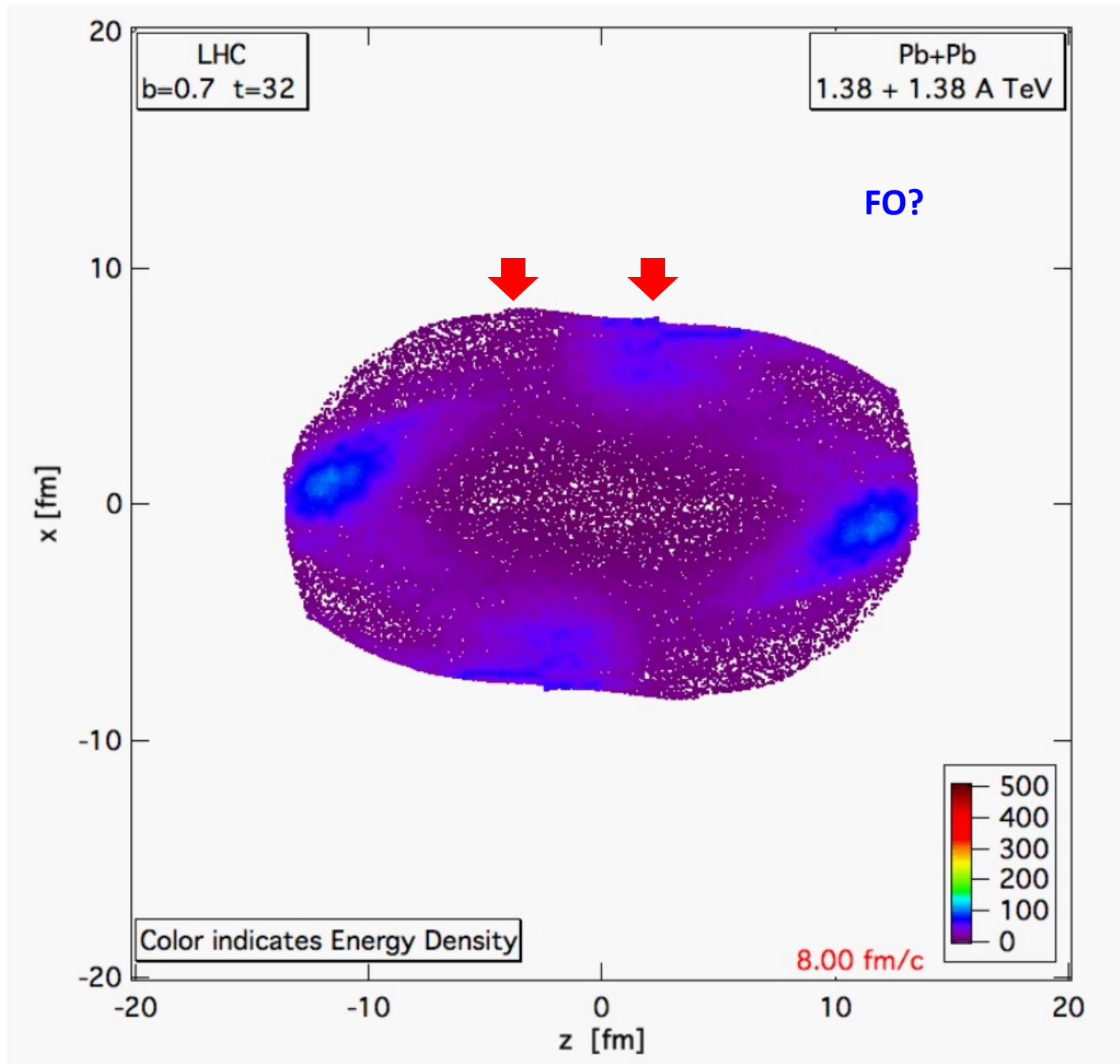
Structure and asymmetries of init. state are maintained in nearly perfect expansion.

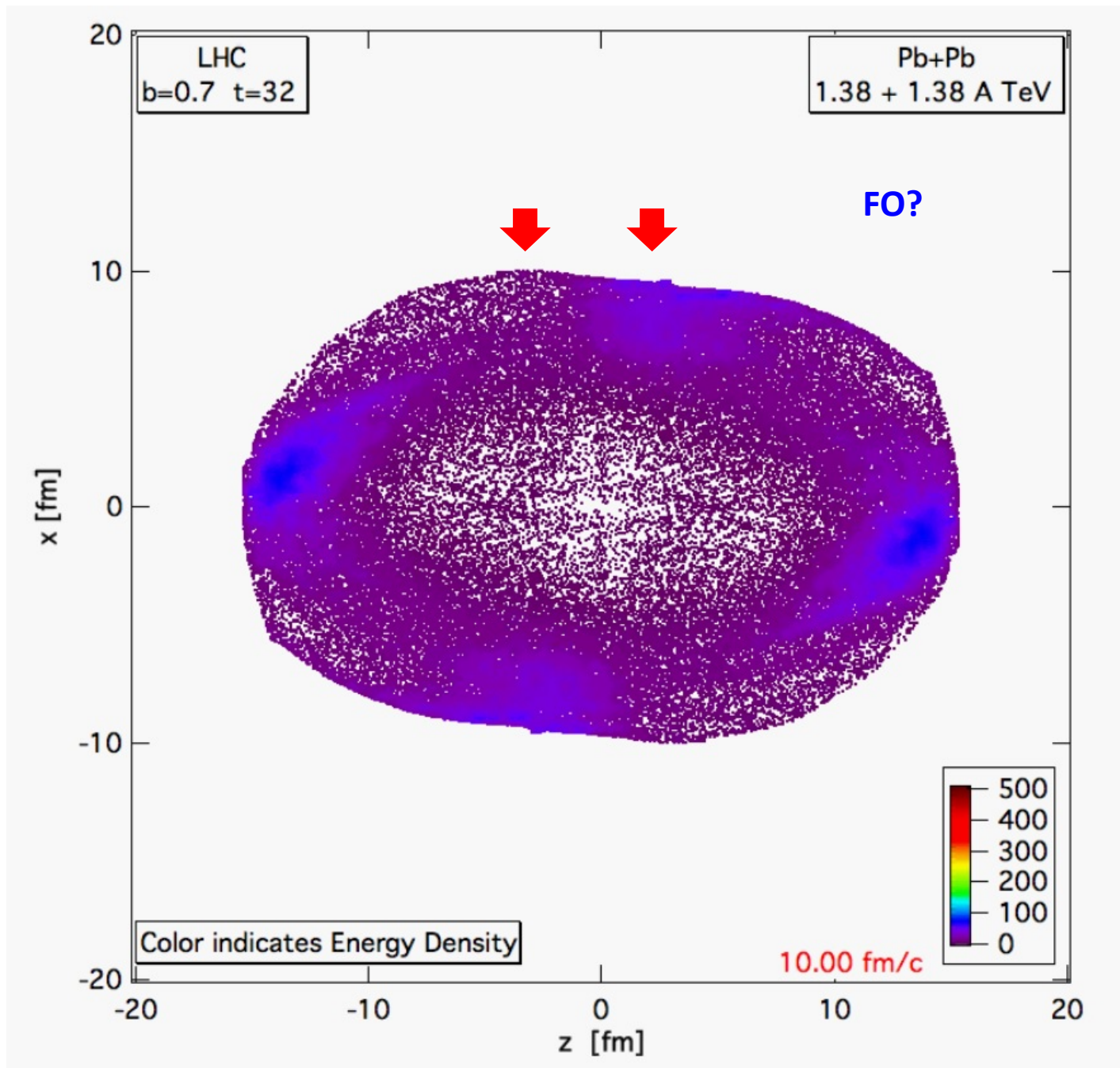
[..\\zz-Movies\\LHC-Ec-1h-b7-A.mov](#)

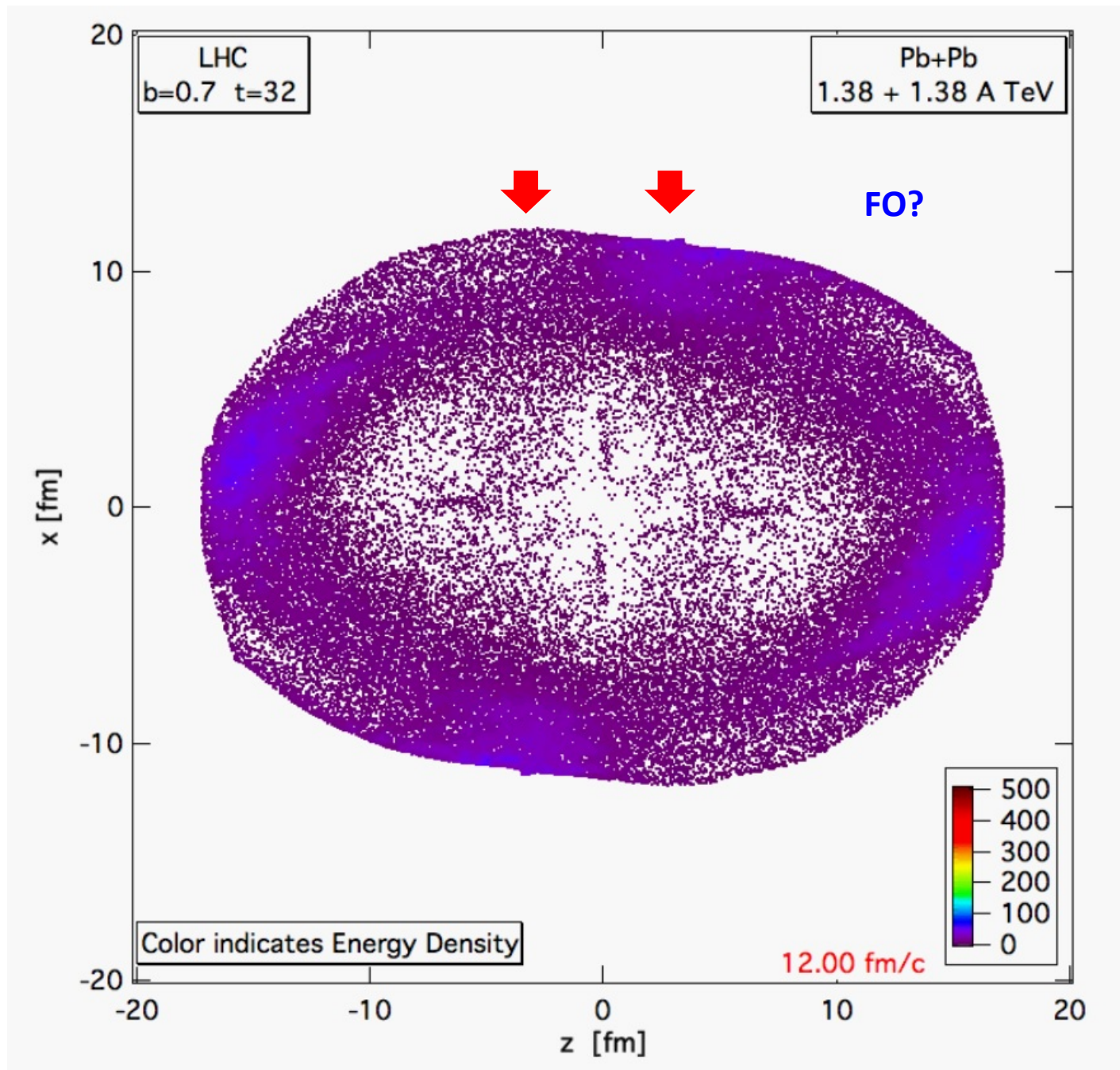


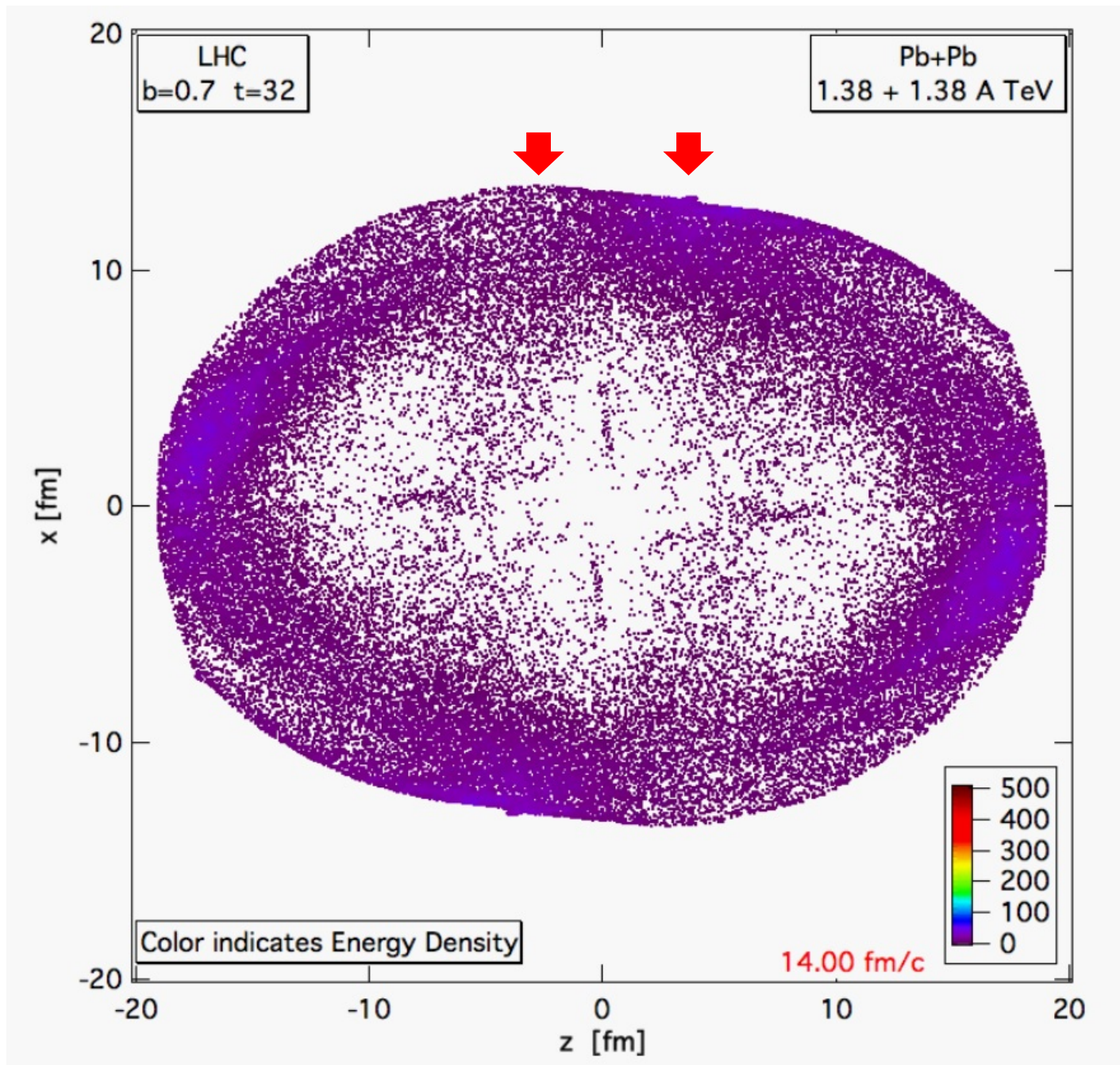


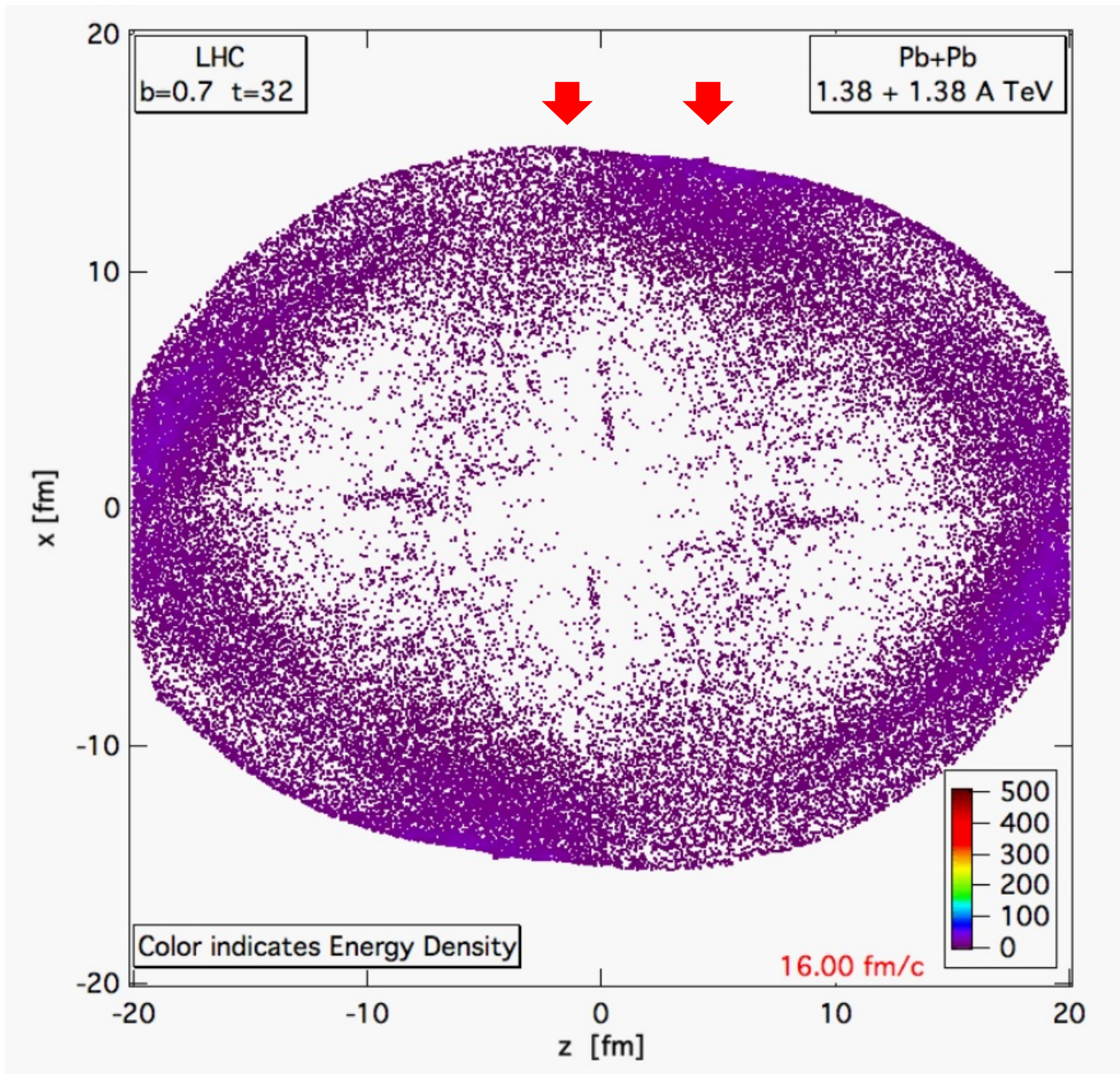




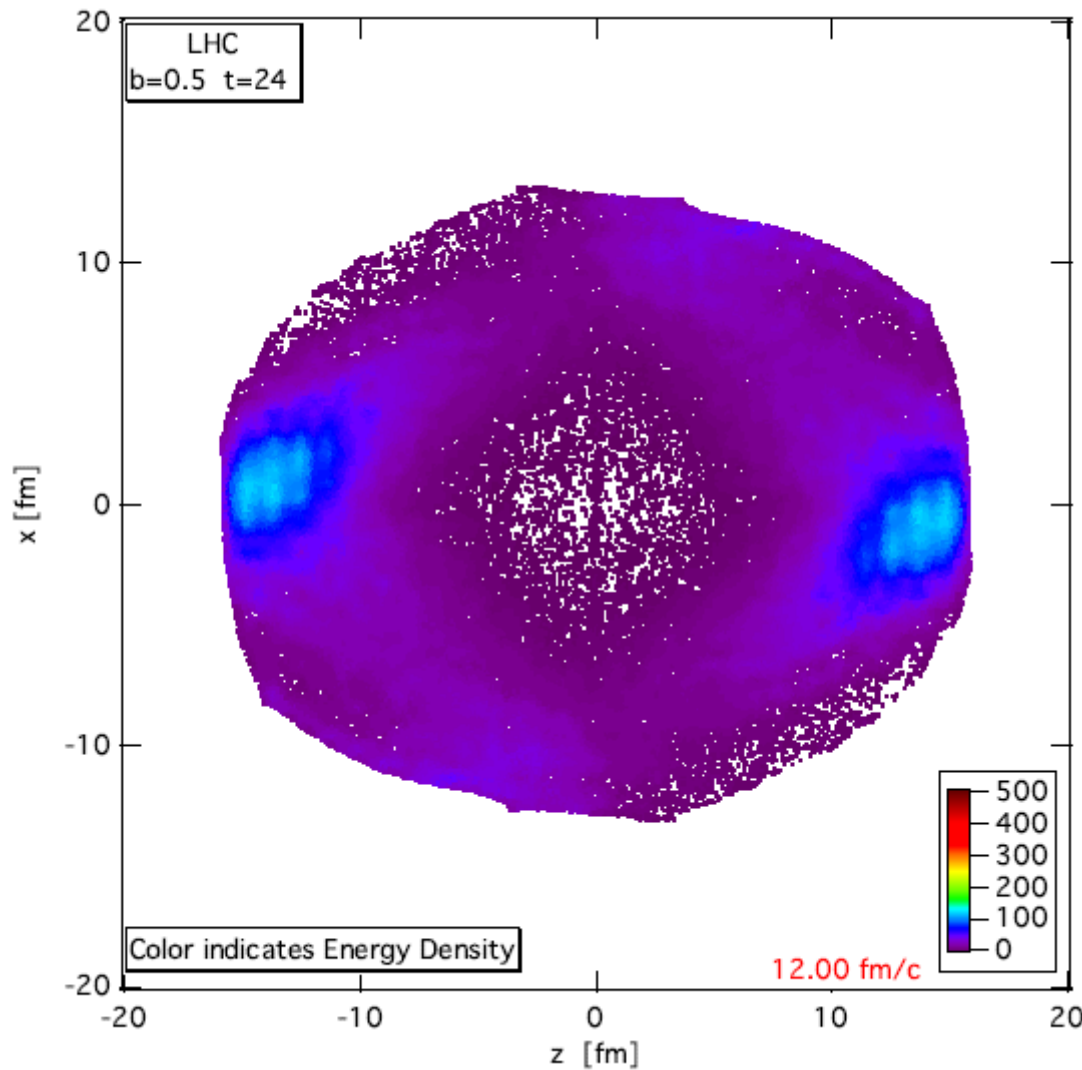








Anti-flow (v_1)

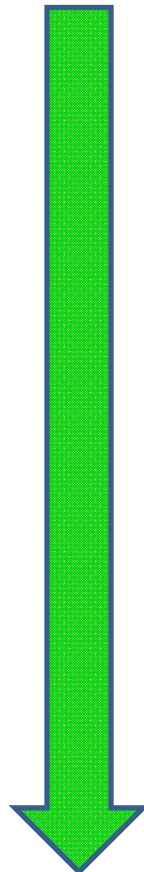


The energy density [GeV/fm³] distribution in the reaction plane, [x,z] for a Pb+Pb reaction at 1.38 + 1.38 A.TeV collision energy and impact parameter $b = 0.5b_{\text{max}}$ at time 12 fm/c after the formation of the hydro initial state. The expected physical FO point is earlier but this post FO configuration illustrates the flow pattern.

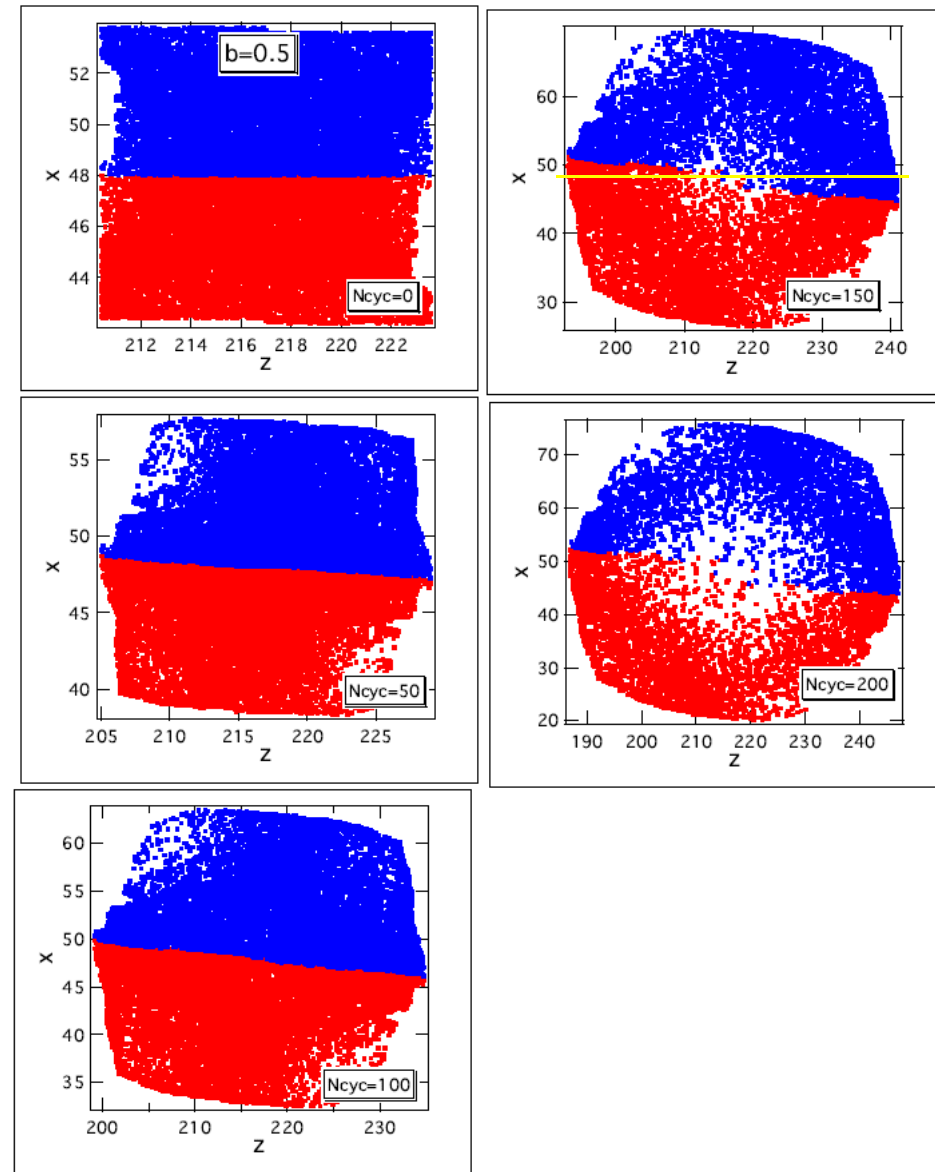
[LP. Csernai, V.K. Magas,
H. Stöcker, D. Strottman,
Phys. Rev. **C84** (2011) 02914]

Rotation

The rotation is illustrated by dividing the upper / lower part (blue/red) of the initial state, and following the trajectories of the marker particles.



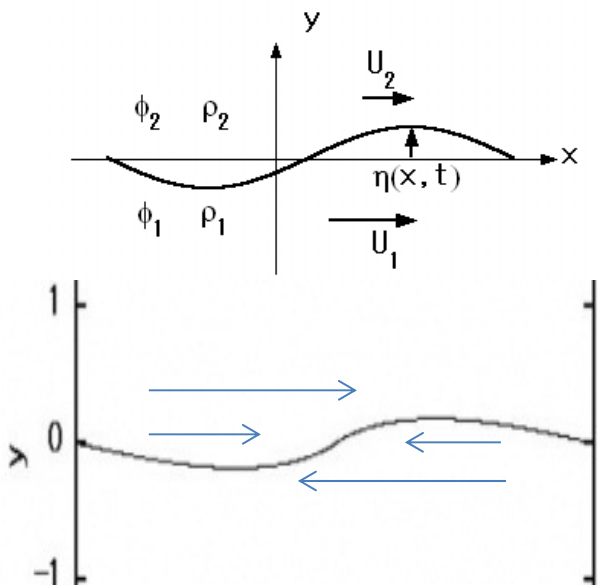
Turbulence ?



The Kelvin – Helmholtz instability at the water surface



- Initial, almost sinusoidal waves, in HI: 10-20 deg. extra rotation.
- Well developed, non-linear wave, not expected in HI collisions!



The interface is a layer with a finite thickness, where viscosity and surface tension affects the interface. Due to these effects singularity formation is prevented in reality. The roll-up of a sheet is observed

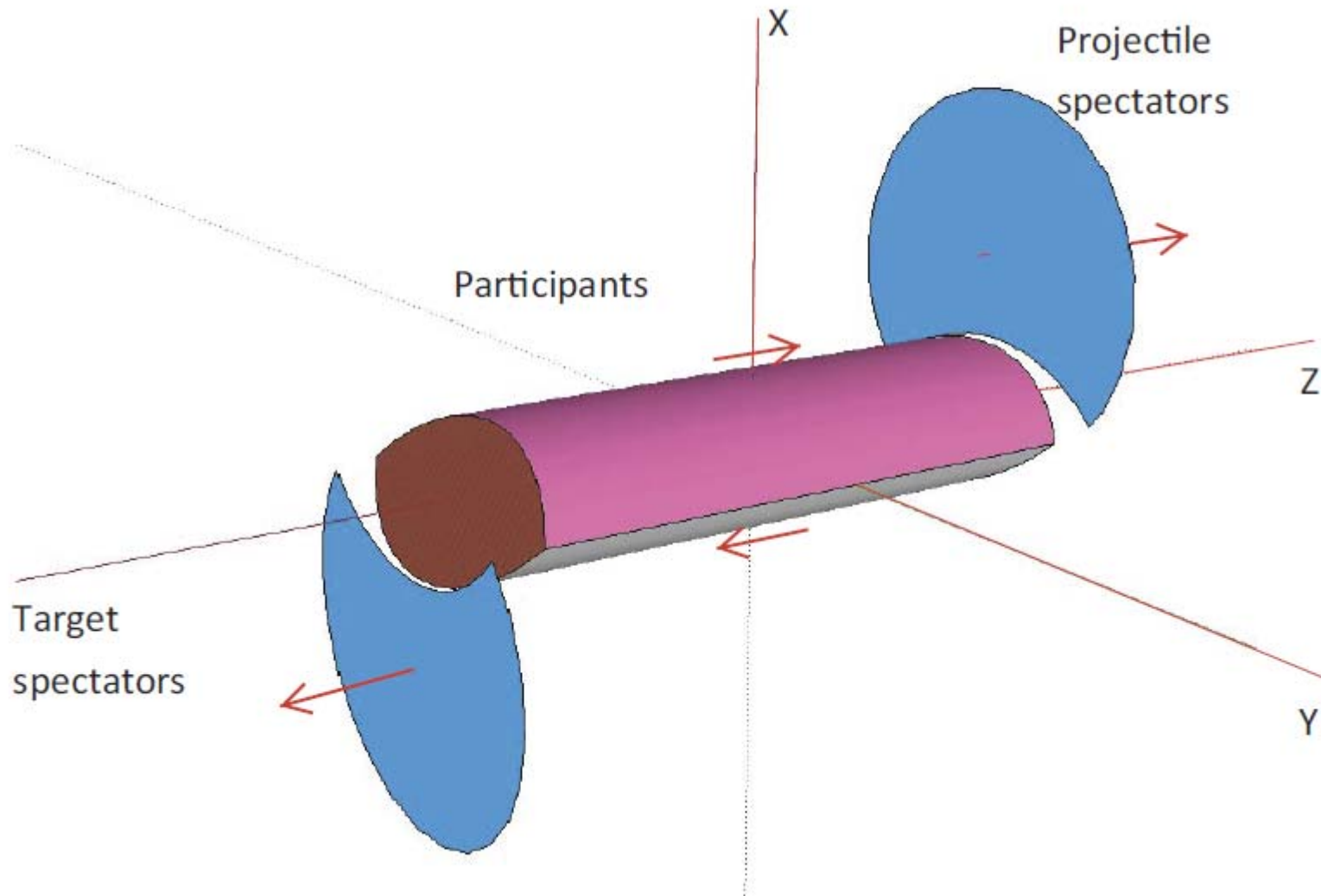


[Chihiro Matsuoka, Yong Guo Shi, Scholarpedia]

The KHI in air from above



Initial geometry at ultra-relativistic energies



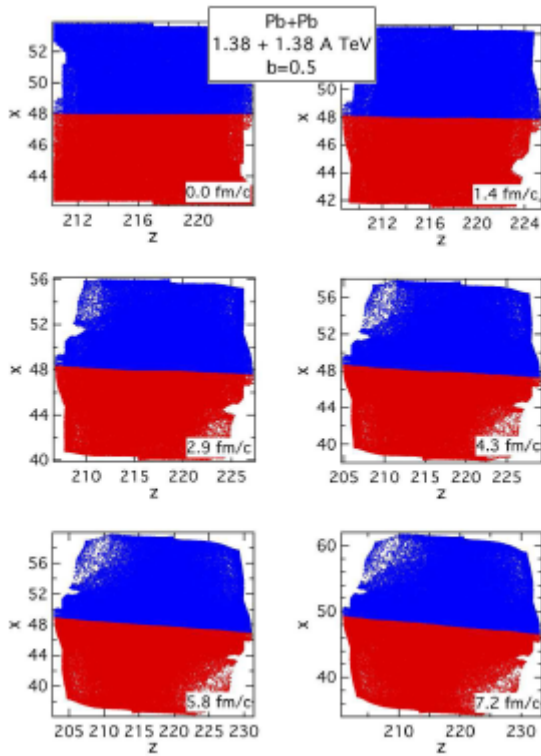
Kelvin-Helmholtz instability in high-energy heavy-ion collisions

L.P. Csernai^{1,2,3}, D.D. Strottman^{2,3}, and Cs. Anderlik⁴

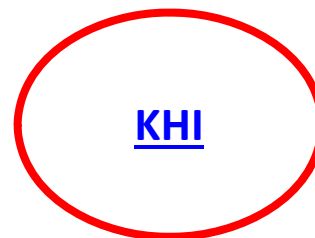
PHYSICAL REVIEW C **85**, 054901 (2012)

arXiv:1112.4287v3 [nucl-th]

ROTATION



KHI →



KHI

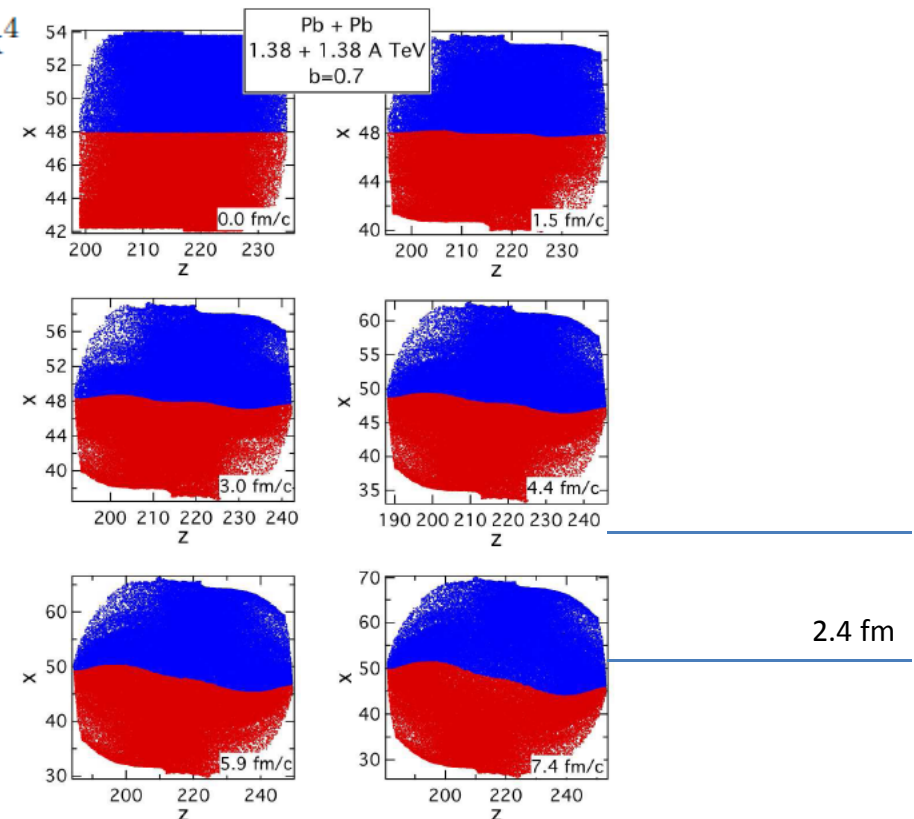
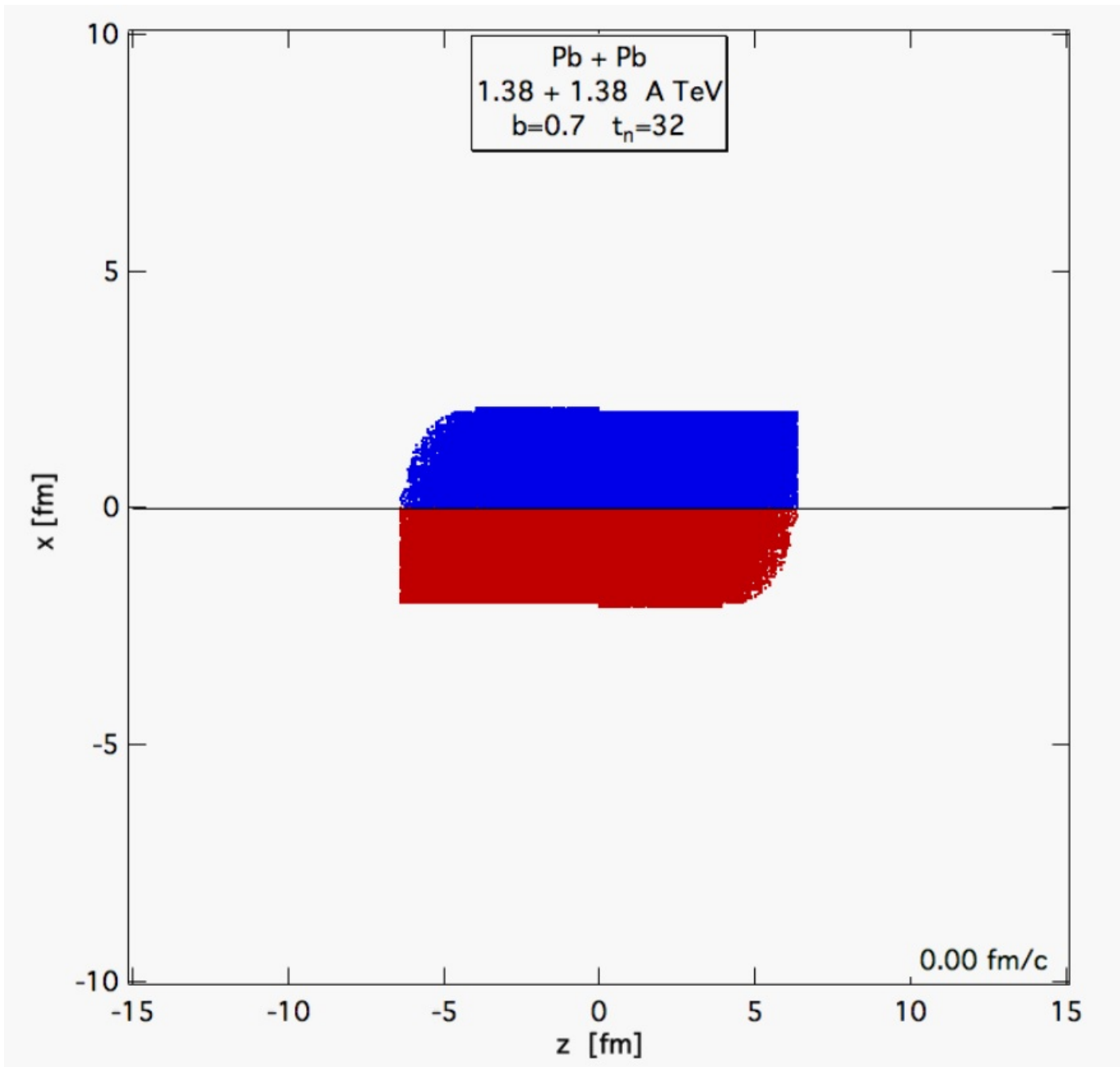
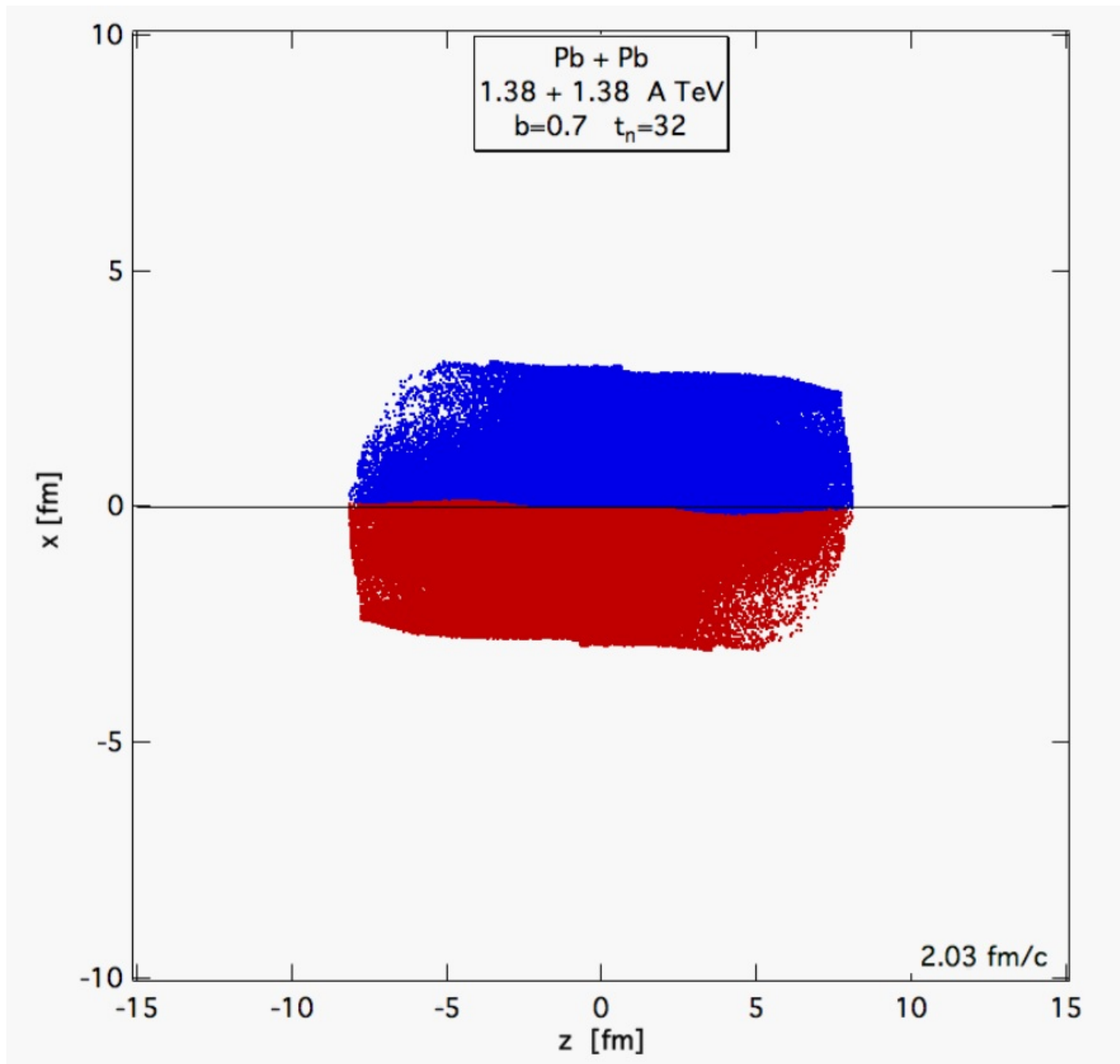
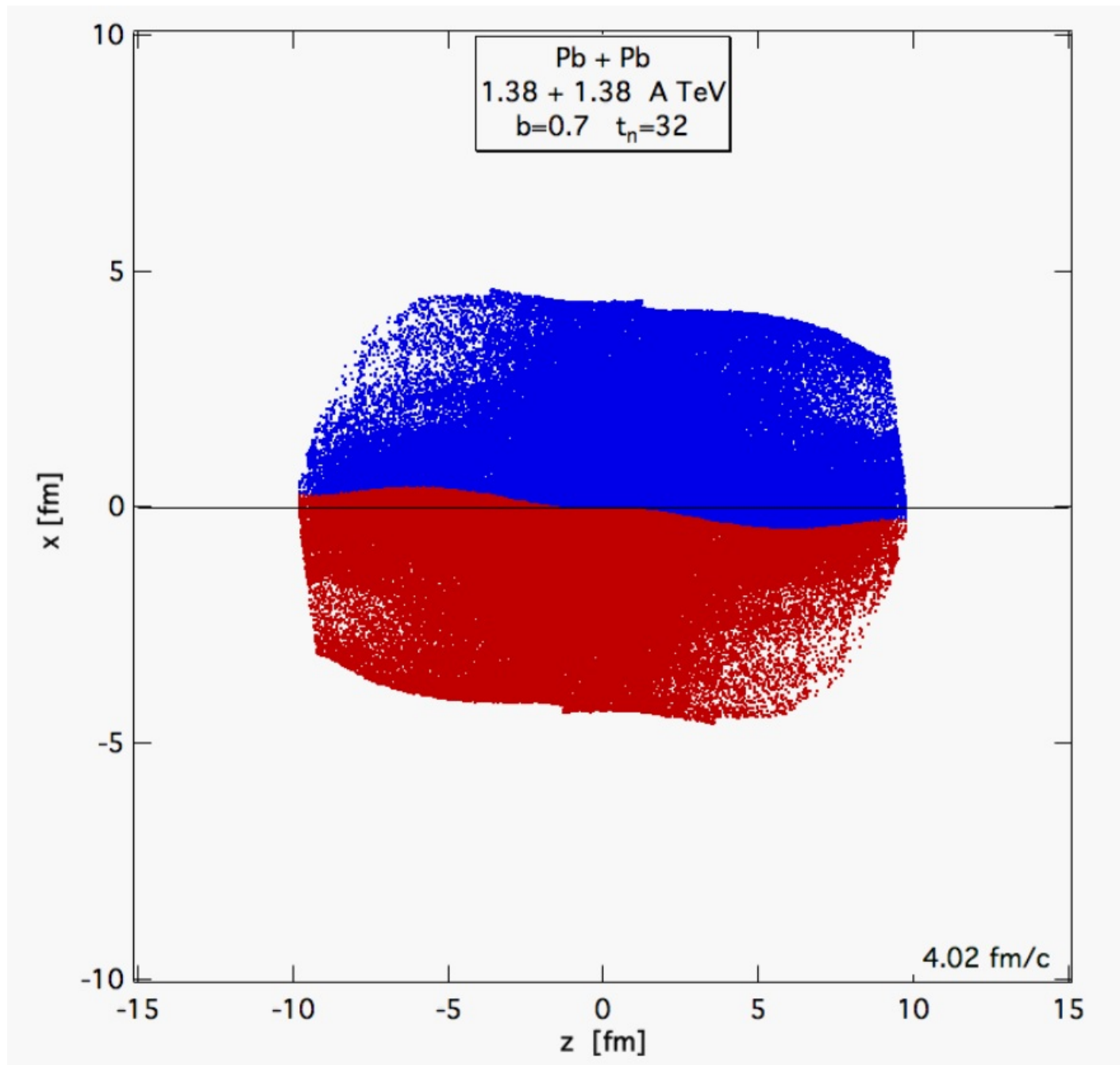
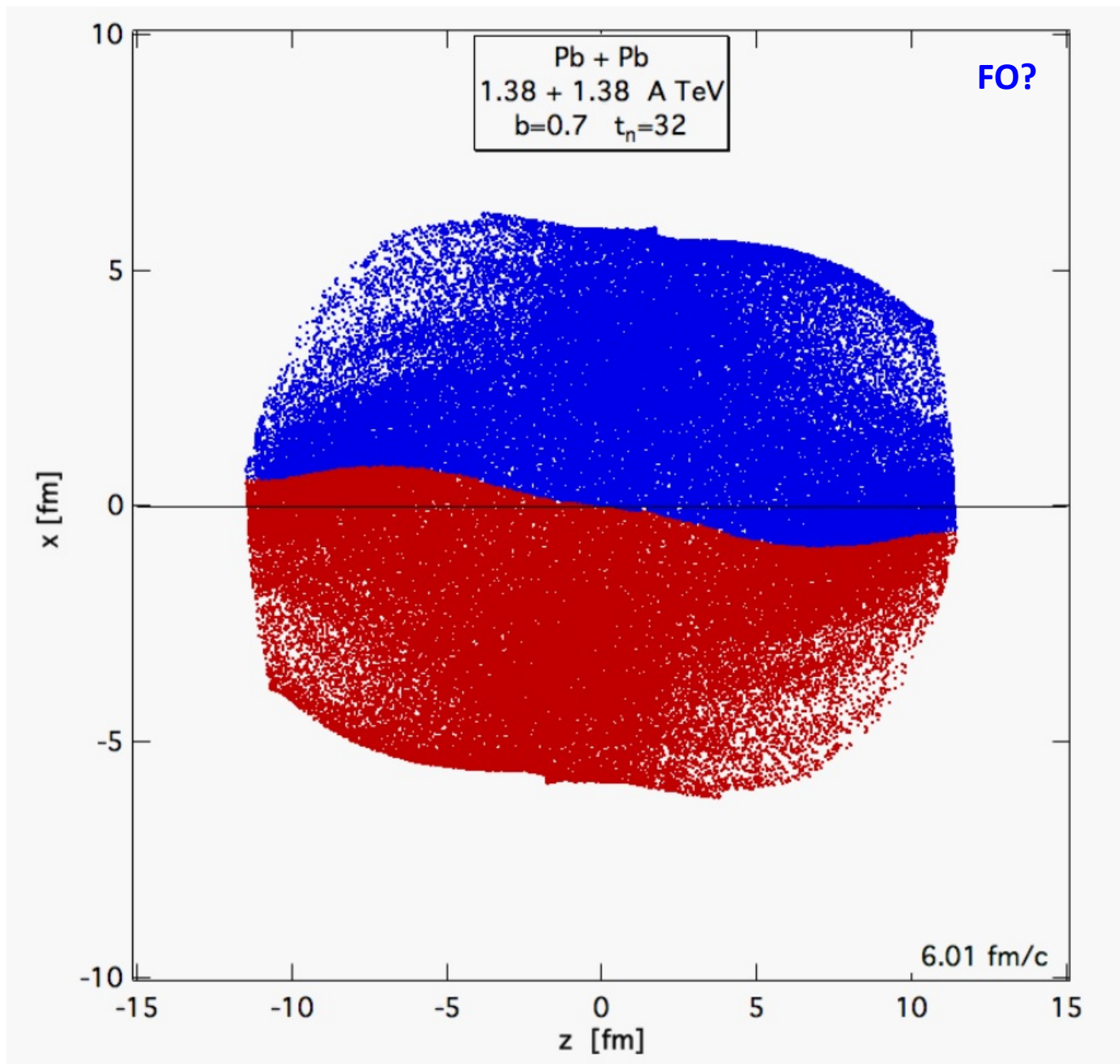


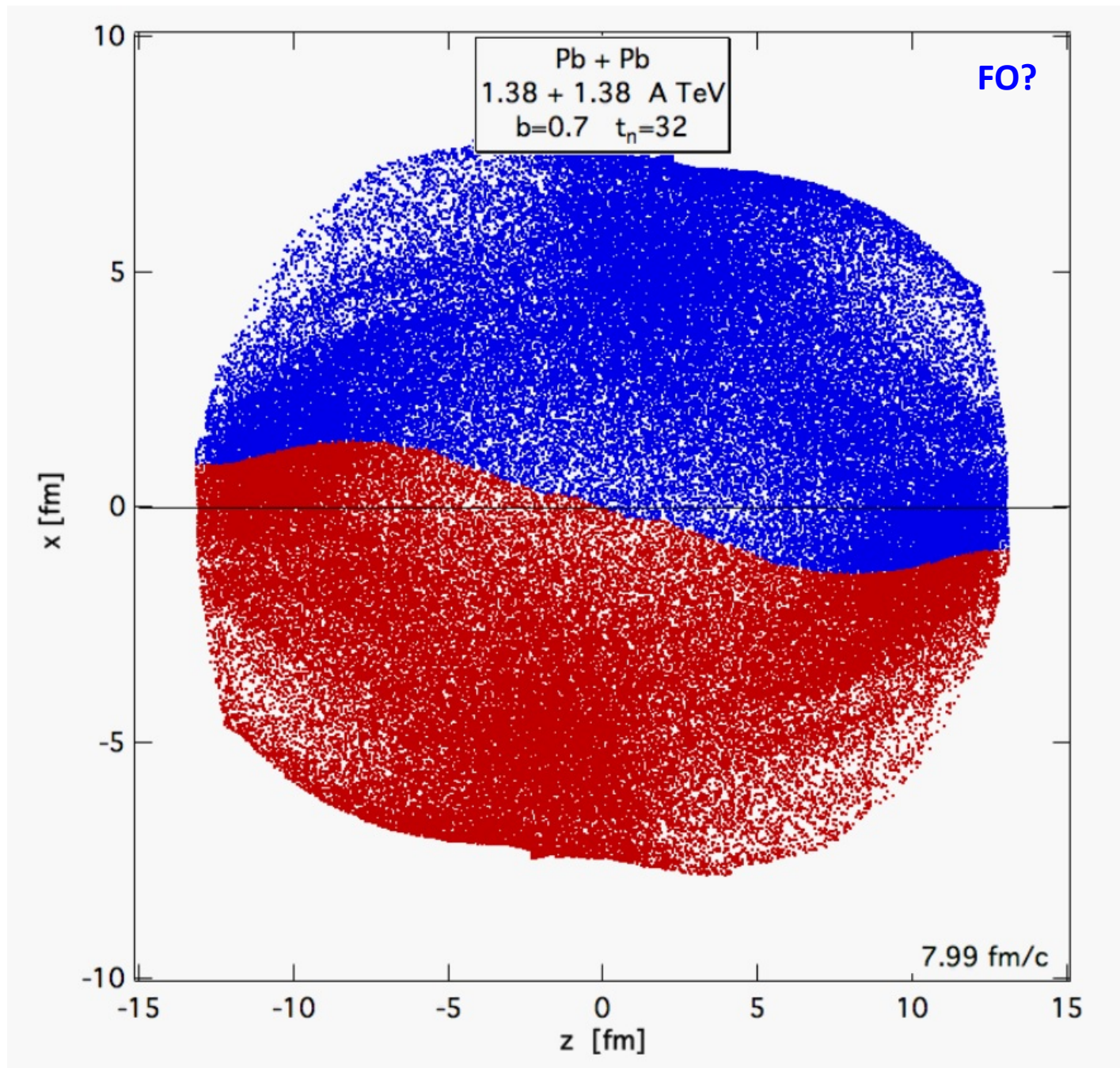
FIG. 1: (color online) Growth of the initial stage of Kelvin-Helmholtz instability in a $1.38A + 1.38A$ TeV peripheral, $b = 0.7b_{\max}$, Pb+Pb collision in a relativistic CFD simulation using the PIC-method. We see the positions of the marker particles (Lagrangian markers with fixed baryon number content) in the reaction plane. The calculation cells are $dx = dy = dz = 0.4375\text{fm}$ and the time-step is $0.04233 \text{ fm}/c$. The number of randomly placed marker particles in each fluid cell is 8^3 . The axis-labels indicate the cell numbers in the x and z (beam) direction. The initial development of a KH type instability is visible from $t = 1.5$ up to $t = 7.41 \text{ fm}/c$ corresponding from 35 to 175 calculation time steps).

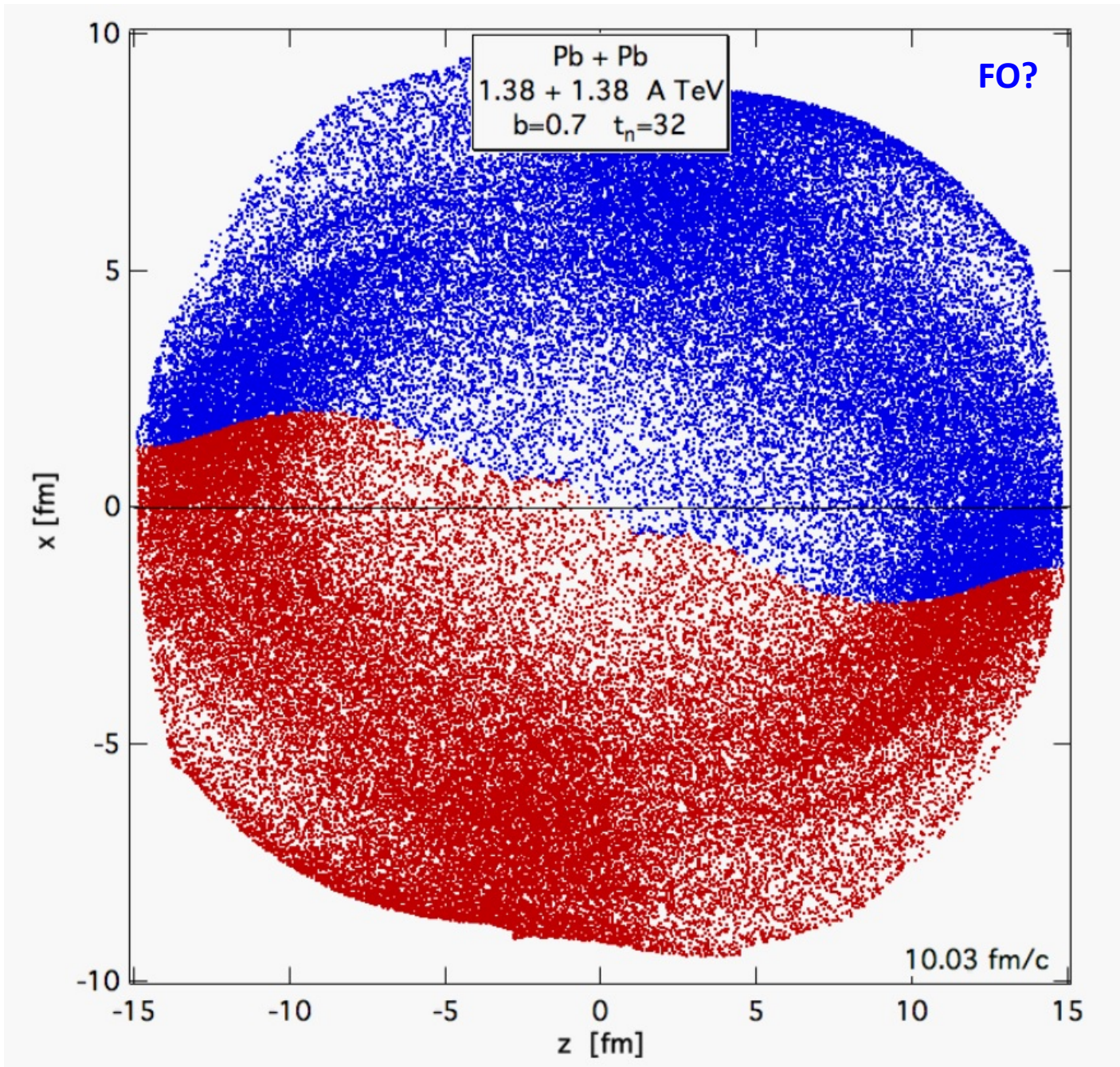




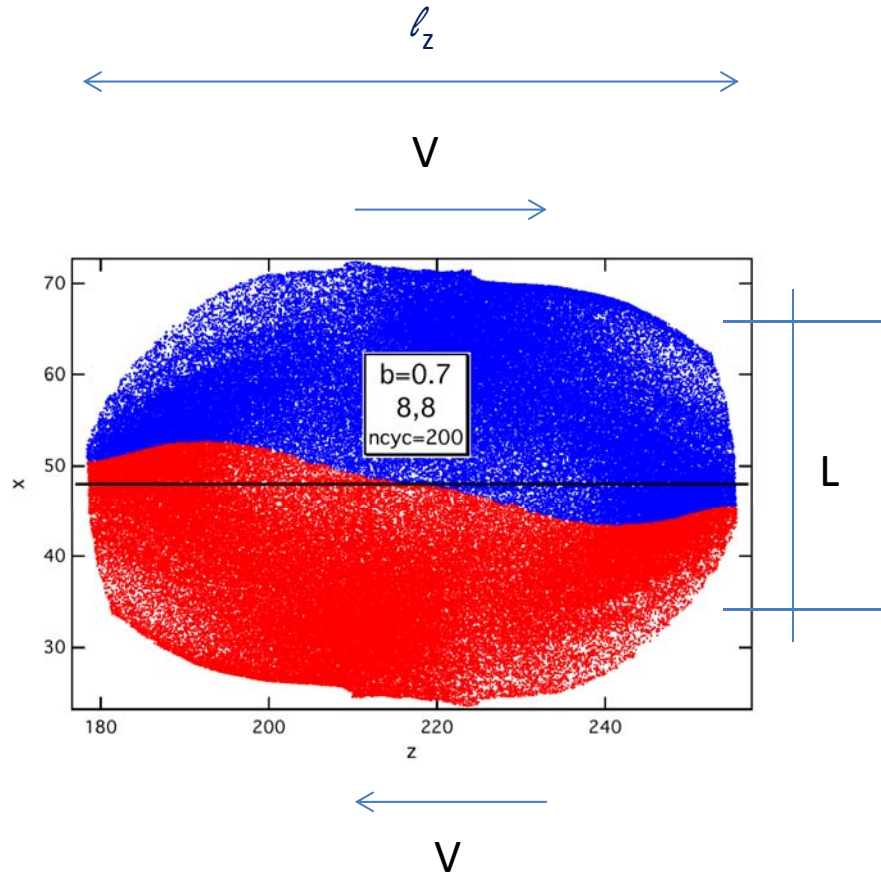








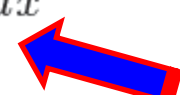
The Kelvin – Helmholtz instability (KHI)



Our resolution is $(0.35\text{fm})^3$ and
 8^3 markers/fluid-cell →
~ 10k cells & 10Mill m.p.-s

- Shear Flow:
- $L=(2R-b) \sim 4 - 7 \text{ fm}$, init. profile height
- $\ell_z = 10 - 13 \text{ fm}$, init. length ($b=.5-.7b_{\max}$)
- $V \sim \pm 0.4 c$ upper/lower speed →
- Minimal wave number is $k = .6 - .48 \text{ fm}^{-1}$
- KHI grows as $\propto \exp(st)$, where $s = kV \rightarrow$
- Largest k or shortest wave-length will grow the fastest.
- The amplitude will double in 2.9 or 3.6 fm/c for ($b=.5-.7b_{\max}$) without expansion, and with favorable viscosity/Reynolds no. $\text{Re}=LV/v$.
- → this favors large L and large V

The Kelvin – Helmholtz instability (KHI)

- Formation of critical length KHI (Kolmogorov length scale)
- \exists critical minimal wavelength beyond which the KHI is able to grow. Smaller wavelength perturbations tend to decay.
(similar to critical bubble size in homogeneous nucleation).
- Kolmogorov: $\lambda_{Kol} = [\nu^3 / \epsilon]^{1/4}$.
- Here $\epsilon = \dot{e}/\rho \propto T\dot{\sigma}/\rho \propto \nu$, ϵ is the specific dissipated flow energy.
- We estimated: $\lambda_{Kol} = \begin{cases} 2.1 \div 5.4 \text{ fm for } b = 0.5b_{max} \\ 1.4 \div 3.6 \text{ fm for } b = 0.7b_{max} \end{cases}$ 
- It is required that $l_z > \lambda_{Kol}$. \rightarrow we need $b > 0.5 b_{max}$
- Furthermore
 - Re = 0.3 – 1 for “ $\eta/s = 1$ ” and
 - Re = 3 – 10 for “ $\eta/s = 0.1$ ”

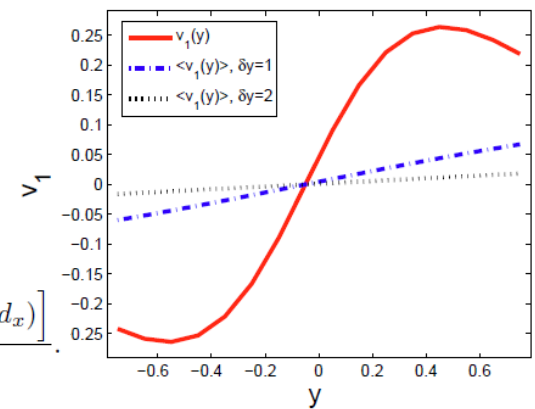
Can we observe rotation and turbulence (KHI) ???

- **v1 peak – From anti-flow towards directed flow:**

PHYSICAL REVIEW C 84, 024914 (2011)

Fluid dynamical prediction of charged v_1 flow at energies available at the CERN Large Hadron Collider

L. P. Csernai,^{1,2,3} V. K. Magas,⁴ H. Stöcker,³ and D. D. Strottman^{1,3}



- **Differential HBT analysis:**

[L.P. Csernai, S. Velle, D.J. Wang] [arXiv:1305.0385](https://arxiv.org/abs/1305.0385), [arXiv:1305.0396](https://arxiv.org/abs/1305.0396)

$$\Delta C(k_{\pm}, q_{out}) \equiv C(k_+, q_{out}) - C(k_-, q_{out}) = \frac{4 \exp(-R^2 q^2) \epsilon \sinh\left(\frac{2u_z b k}{T_s}\right) (1-\epsilon^2) \left[1 - \cosh\left(\frac{u_z b q}{T_s}\right) \cos(aqd_x) \right]}{\left[(1+\epsilon^2) \cosh\left(\frac{2u_z b k}{T_s}\right) + (1-\epsilon^2) \right]^2 - 4\epsilon^2 \sinh^2\left(\frac{2u_z b k}{T_s}\right)}.$$

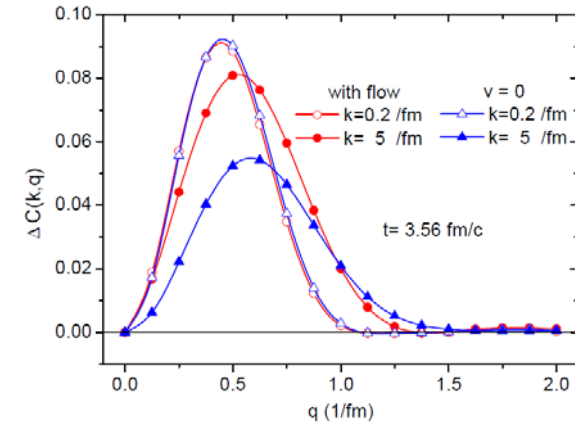
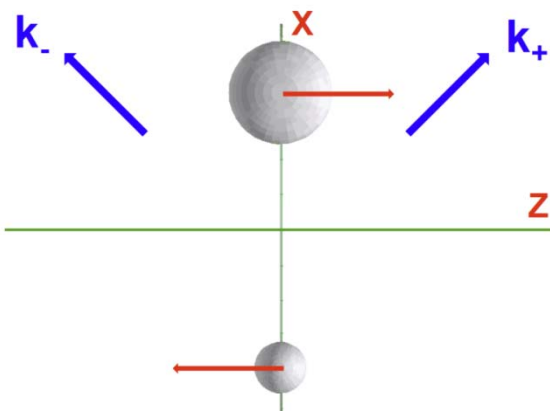


FIG. 3. (color online) The flow velocity dependence of the differential correlation function at the final time.

- **POLARIZATION of Λ and $\bar{\Lambda}$ due to thermal equipartition with local vorticity.**

Local vorticity

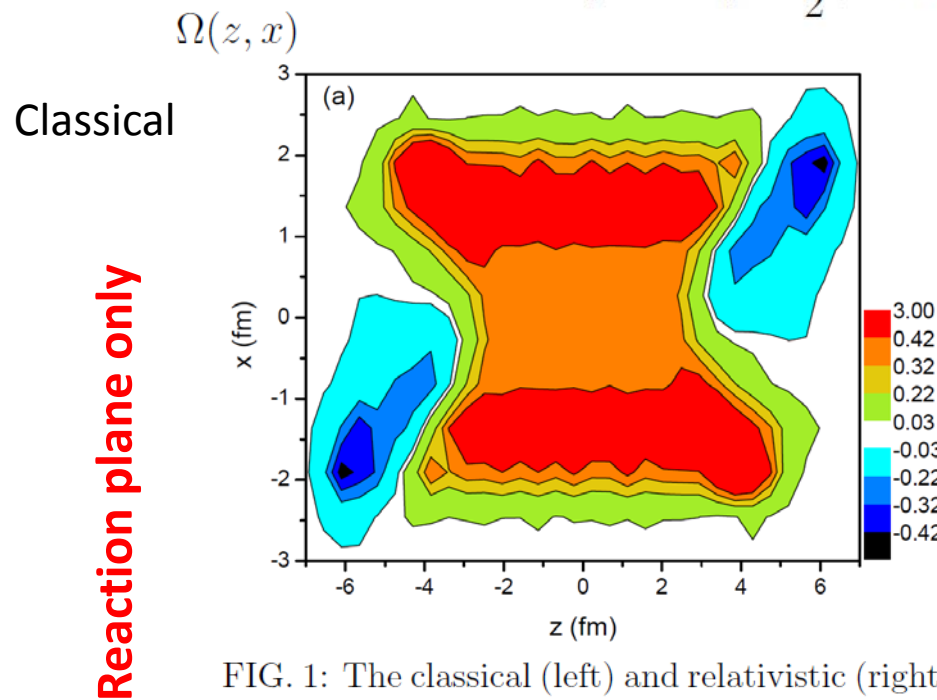
PHYSICAL REVIEW C 87, 034906 (2013)

Flow vorticity in peripheral high-energy heavy-ion collisions

L. P. Csernai,¹ V. K. Magas,² and D. J. Wang¹

$$\omega_y \equiv \omega_{xz} \equiv \frac{1}{2}(\partial_z v_x - \partial_x v_z)$$

$$\omega_z^x = -\omega_x^z = \frac{1}{2}(\partial_z \gamma v_x - \partial_x \gamma v_z) = \frac{1}{2}\gamma(\partial_z v_x - \partial_x v_z) + \frac{1}{2}(v_x \partial_z \gamma - v_z \partial_x \gamma)$$



$$\Omega(z, x) \equiv w(z, x)\omega(z, x)$$

$$w_{ik} \equiv (N_{cell}/E_{tot}) E_{ik}.$$

$$\Theta \equiv \nabla_\mu u^\mu = \partial_\mu u^\mu,$$

$$\omega_\nu^\mu \equiv \frac{1}{2}(\nabla_\nu u^\mu - \nabla^\mu u_\nu),$$

If $\partial_\tau u^\mu \equiv \dot{u}^\mu = u^\alpha \partial_\alpha u^\mu$ is negligible

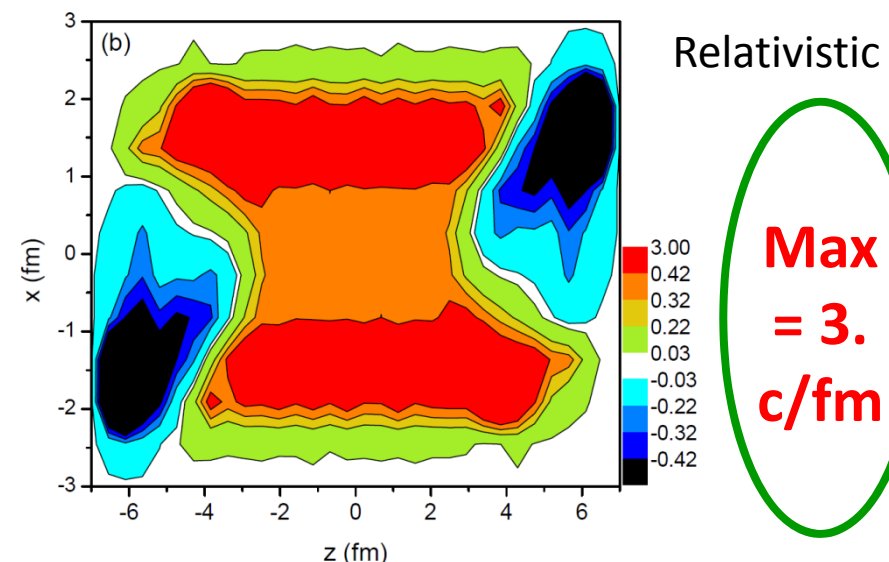


FIG. 1: The classical (left) and relativistic (right) weighted vorticity, Ω_{zx} , calculated in the reaction, [x-z] plane at $t=0.17$ fm/c. The collision energy is $\sqrt{s_{NN}} = 2.76$ TeV and $b = 0.7b_{max}$, the cell size is $dx = dy = dz = 0.4375$ fm. The average vorticity in the reaction plane is 0.1434 / 0.1185 for the classical / relativistic weighted vorticity respectively.

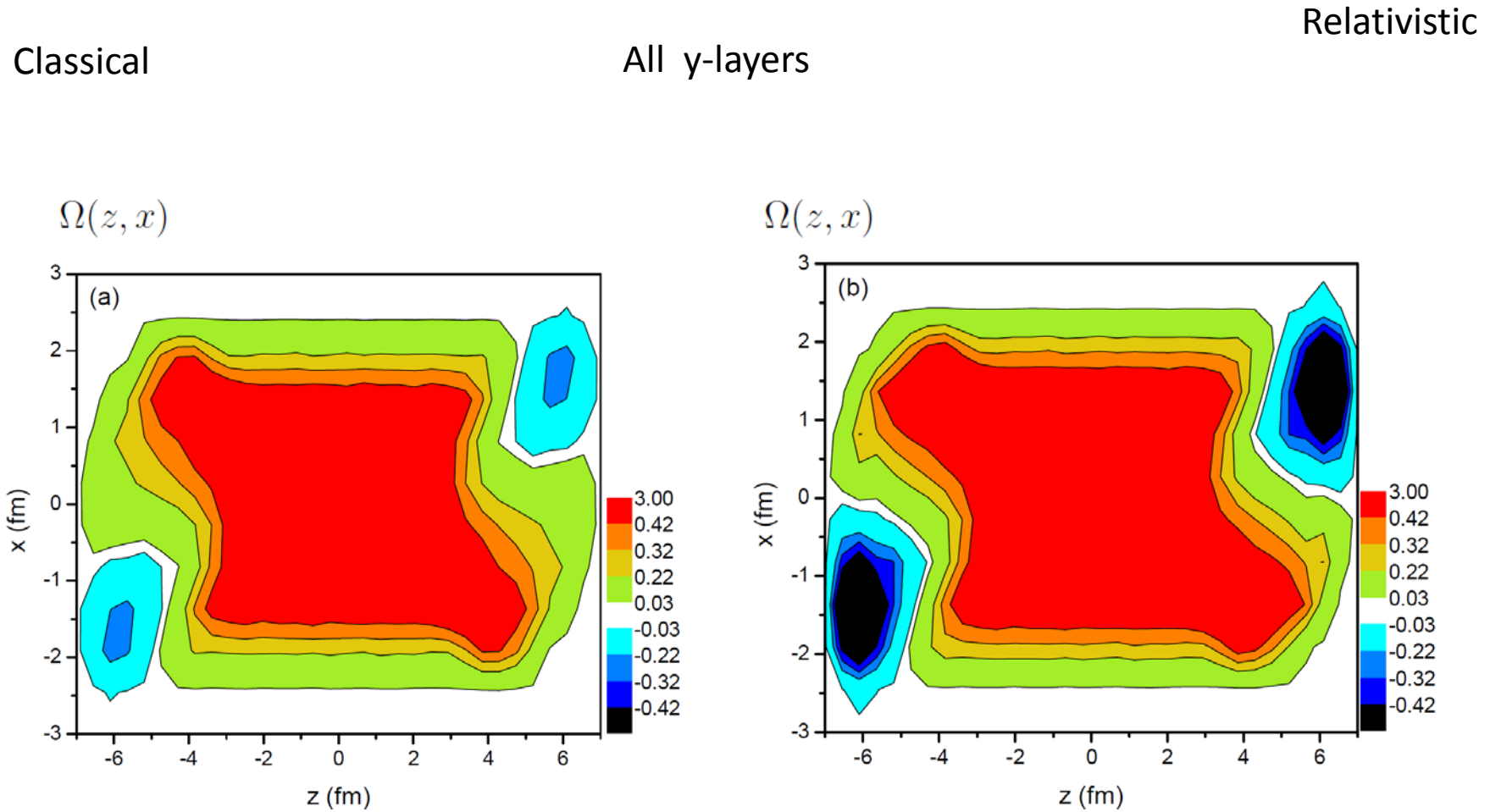


FIG. 4: The classical (left) and relativistic (right) weighted vorticity calculated for all [x-z] layers at $t=0.17$ fm/c. The collision energy is $\sqrt{s_{NN}} = 2.76$ TeV and $b = 0.7b_{max}$, the cell size is $dx = dy = dz = 0.4375$ fm.

the surface element $S(t)$. Then we can describe the *circulation* along

$$\Gamma(C(t)) = \oint_{C(t)} \mathbf{v} \cdot d\mathbf{l} = \int \int_{S(t)} \vec{\omega} \cdot \mathbf{n} \, dS$$

where ω is the vorticity

$$\vec{\omega} = \text{rot } \mathbf{v}$$

The circulation is conserved for perfect incompressible classical fluids.

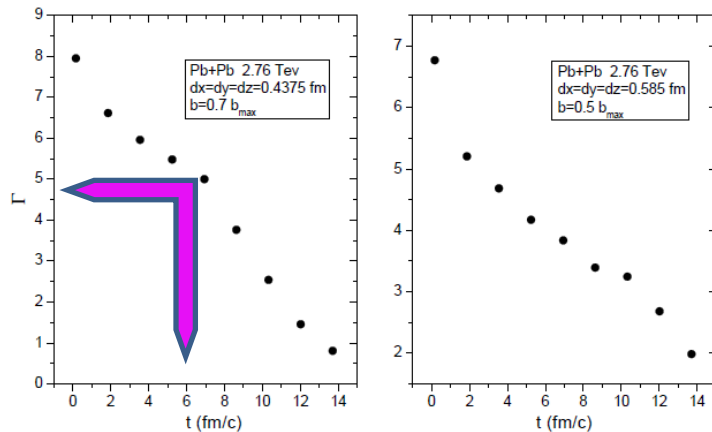
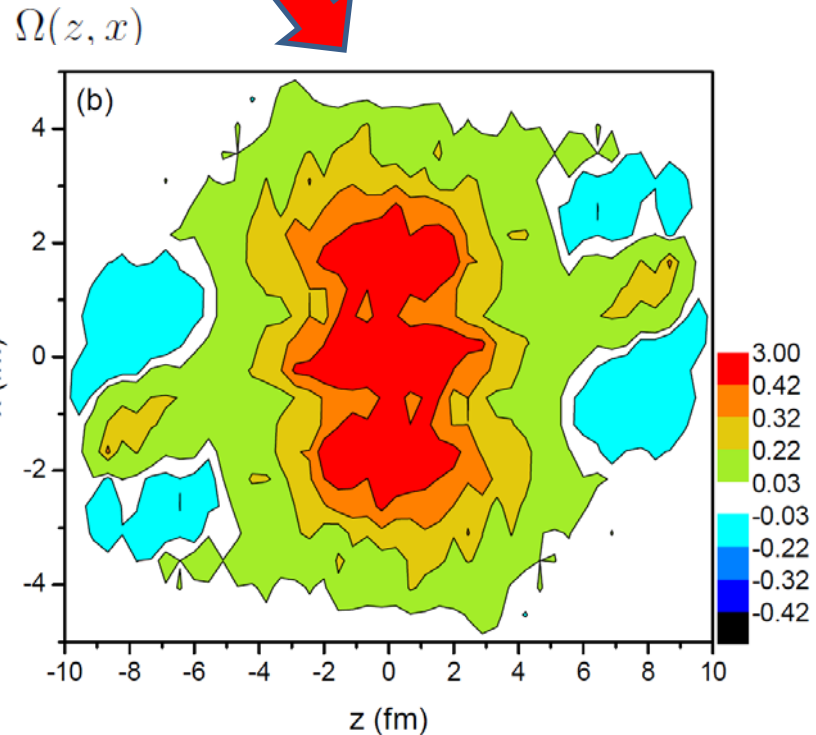
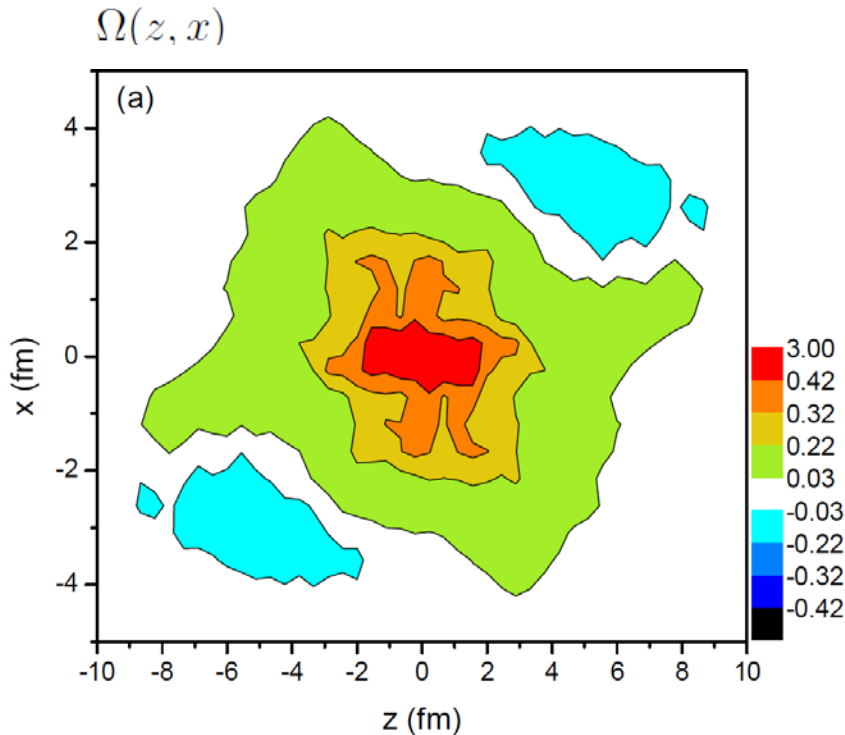


FIG. 7: The time dependence of classical circulation, $\Gamma(t)$, in units of [fm c], calculated for all [x-z] layers and then taking the average of the circulations for all layers. The collision energy is $\sqrt{s_{NN}} = 2.76$ TeV and $b = 0.7b_{max}$, the cell size is $dx = dy = dz = 0.4375\text{fm}$ (left). For comparison another initial state configuration was also tested for the same collision energy but $b = 0.5b_{max}$, the cell size is $dx = dy = dz = 0.585\text{fm}$ (right). This configuration shows also the rotation, but due to its less favorable parameters it does not show the KHI. Although at this impact parameter, which is less peripheral the reaction plane has a larger area filled with matter, nevertheless the initial classical circulation is less by about 15%. For the more peripheral case with smaller numerical viscosity the circulation decreases with time faster and the circulation for the two cases becomes equal around $t = 10\text{ fm/c}$.

Standard Flow Vorticity

Classical



Relativistic

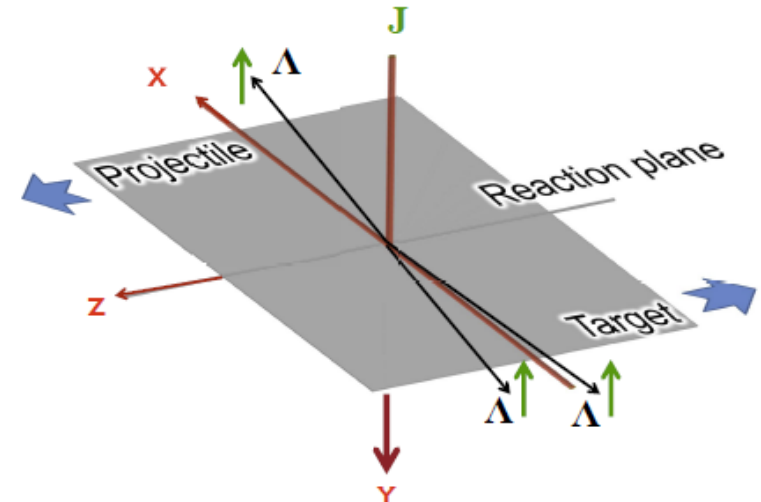
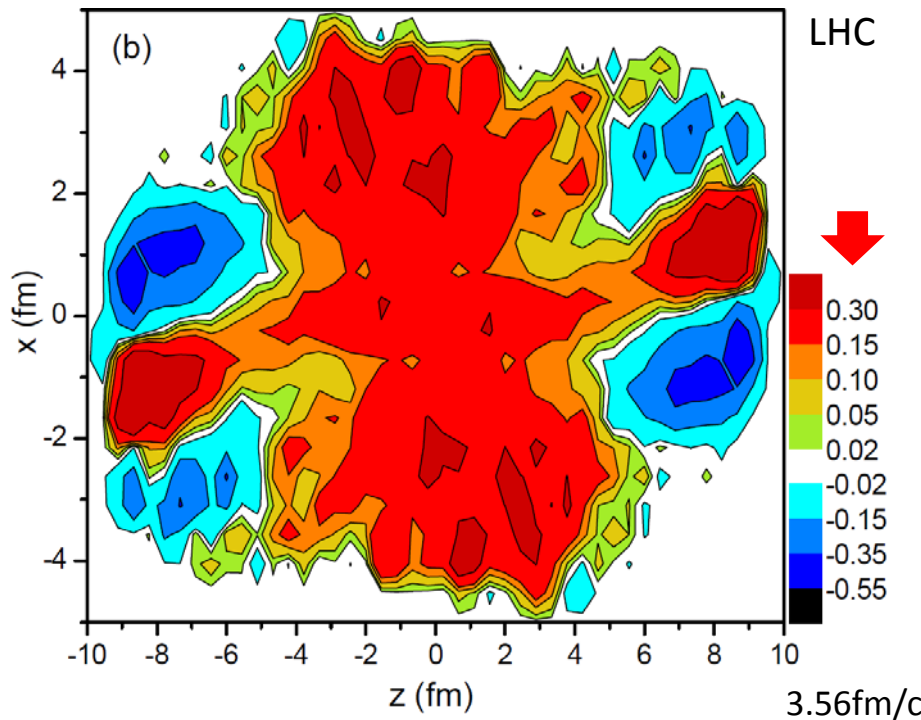
FIG. 5: The classical (left) and relativistic (right) weighted vorticity calculated for all [x-z] layers at $t=3.56$ fm/c. The collision energy is $\sqrt{s_{NN}} = 2.76$ TeV and $b = 0.7b_{max}$, the cell size is $dx = dy = dz = 0.4375$ fm. The average vorticity in the reaction plane is 0.0538 / 0.10685 for the classical / relativistic weighted vorticity respectively.

Detecting rotation: Lambda polarization

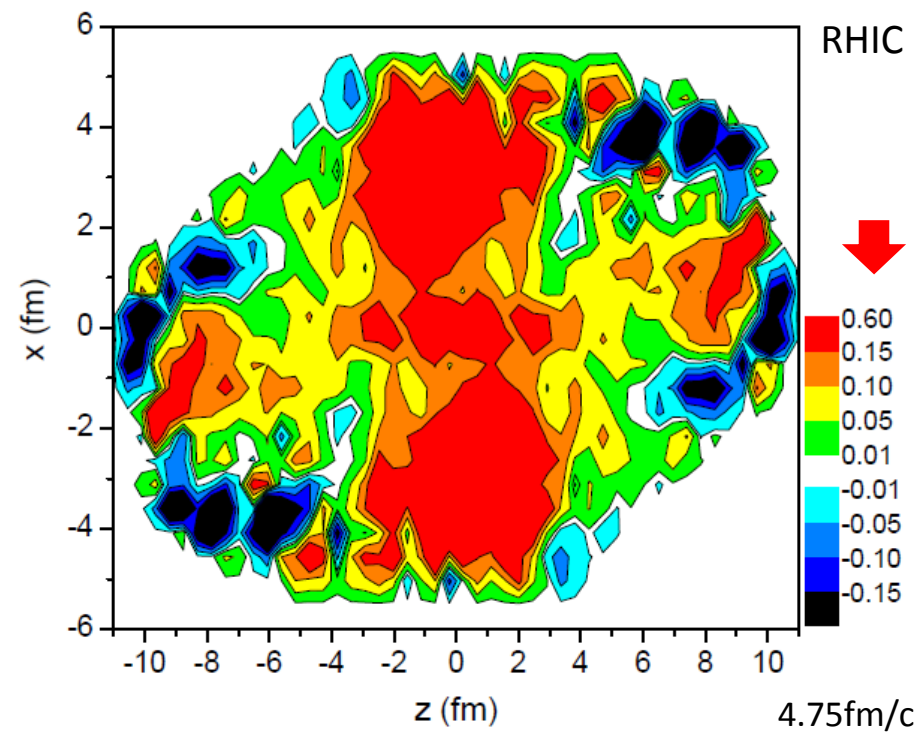
$$\Pi(p) = \frac{\hbar \varepsilon}{8m} \frac{\int dV n_F (\nabla \times \beta)}{\int dV n_F}$$

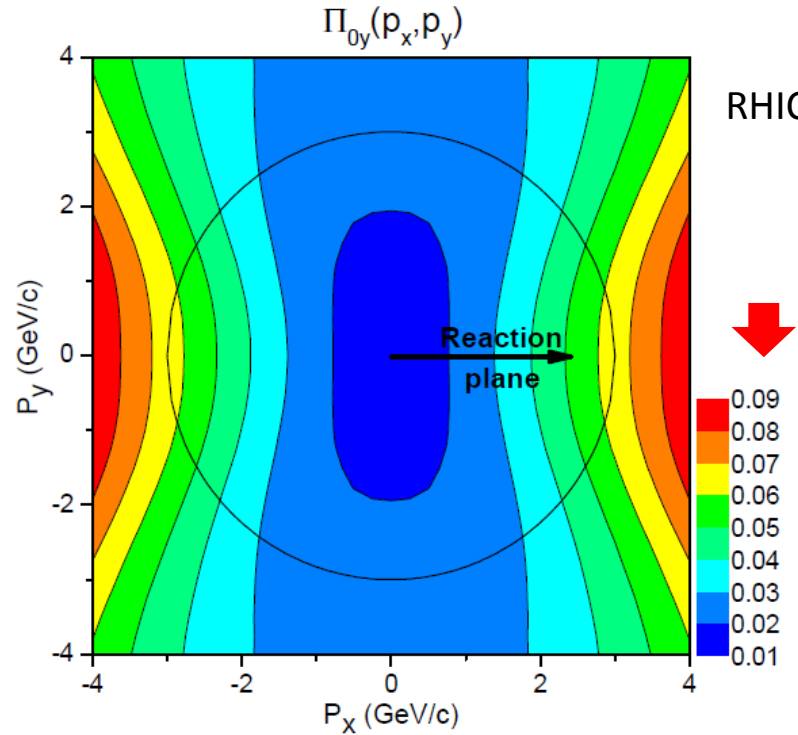
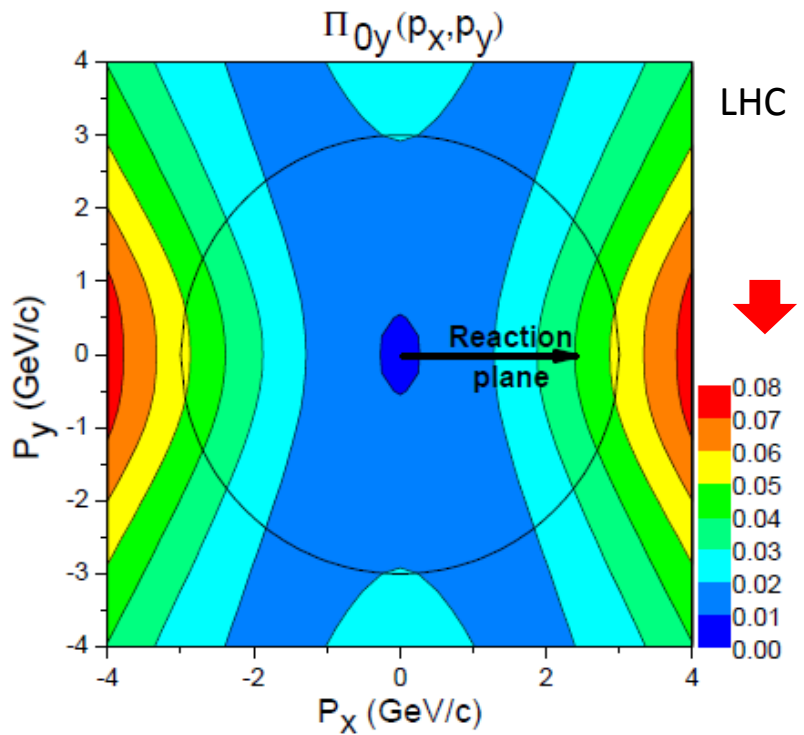
$$\beta^\mu(x) = (1/T(x))u^\mu(x) \quad \leftarrow \text{From hydro}$$

$$\Pi_0(p) = \Pi(p) - \frac{\mathbf{p}}{\varepsilon(\varepsilon + m)} \Pi(p) \cdot \mathbf{p}$$



[F. Becattini, L.P. Csernai, D.J. Wang,
arXiv:1304.4427v1 /nucl-th]





- The **POLARIZATION** of Λ and $\bar{\Lambda}$ due to thermal equipartition with local vorticity is slightly stronger at RHIC than at LHC due to the much higher temperatures at LHC.
- Although early measurements at RHIC were negative, these were averaged over azimuth! We propose selective measurement in the reaction plane (in the +/- x direction) in the EbE c.m. frame. Statistical error is much reduced now, so significant effect is expected at $p_x \geq 3$ GeV/c.

Summary

- In A+A the I.S. is causing global collective flow.
- Consistent I.S. is needed based on a dynamical picture, satisfying causality, etc.
- Low viscosity at peripheral reactions may lead to increased rotation, shear, vorticity and turbulence.
- These lead to measurable consequences, as modified v_1 flow and special HBT behavior.
- Most interestingly mechanical and thermal equilibration may convert the large initial angular momentum to particle polarization.

Thank you

